Antarctic Science 8 (1): 85–104 (1996)

Geochemistry and origin of Mesoproterozoic metavolcanic rocks from Fisher Massif, Prince Charles Mountains, East Antarctica

E. V. MIKHALSKY[1], J. W. SHERATON[2], A. A. LAIBA[3] and B. V. BELIATSKY[1]

[1]VNIIOkeangeologia, Maklina 1, St Petersburg 190121, Russia
[2]Australian Geological Survey Organisation, PO Box 378, Canberra, ACT 2601, Australia
[3]Polar Marine Geological Research Expedition, Pobedy 24, Lomonosov, St Petersburg 189510, Russia

Abstract: Fisher Massif consists of Mesoproterozoic (*c.*1300 Ma) lower amphibolite-facies metavolcanic rocks and associated metasediments, intruded by a variety of subvolcanic and plutonic bodies (gabbro to granite). It differs in both composition and metamorphic grade from the rest of the northern Prince Charles Mountains, which were metamorphosed to granulite facies about 1000 m.y. ago. The metavolcanic rocks consist mainly of basalt, but basaltic andesite, andesite, and more felsic rocks (dacite, rhyodacite, and rhyolite) are also common. Most of the basaltic rocks have compositions similar to low-K island arc tholeiites, but some are relatively Nb-rich and more akin to P-MORB. Intermediate to felsic medium to high-K volcanic rocks, which appear to postdate the basaltic succession, have calc-alkaline affinities and probably include a significant crustal component. On the present data, an active continental margin with associated island arc was the most likely tectonic setting for generation of the Fisher Massif volcanic rocks.

Recieved 9 December 1994, accepted 7 July 1995

Key words: volcanic rocks, basalt, island arc, geochemistry, Proterozoic, Antarctica

Introduction

The central part of East Antarctica between 60° and 80°E comprises three distinctive tectonic provinces: the Archaean Vestfold Hills, the Archaean southern Prince Charles Mountains (SPCM), and an extensive Mesoproterozoic mobile belt (PMB) separating these cratonic blocks (Fig. 1) (Oliver *et al.* 1982, Tingey 1982, Collerson & Sheraton 1986, Black *et al.* 1992, Kamenev 1993). A number of published works on the structure and composition of the Vestfold Hills and adjacent parts of the PMB (Rauer Islands and Prydz Bay area) described their metamorphic and tectonic histories in some detail and put constraints on their upper crustal structure and evolution (Sheraton & Collerson 1984, Harley 1988, Stüwe & Powell 1989, Stüwe *et al.* 1989, Fitzsimons & Harley 1992, Harley *et al.* 1992). Isotopic evidence from the Larsemann Hills area suggests that high-grade metamorphism there was of Pan-African (*c.* 500 Ma) age (Zhao *et al.* 1992, Hensen & Zhou 1995). In contrast, the geological relationships of the Archaean SPCM terrane (Ruker Terrane, RT, of Kamenev 1993) with the PMB are poorly understood, due to a lack of detailed structural, geochemical and isotopic studies. The SPCM was the subject of reconnaissance geological studies in 1954–56 (Crohn 1959, McLeod 1964), and regional mapping by Australian National Antarctic Research Expeditions (ANARE) in 1972–74 (Tingey 1974, 1982) and by Soviet Antarctic Expeditions (SAE) in 1972–75 (Ravich *et al.* 1984) and 1984–91 (Kamenev *et al.* 1993). Archaean granite and felsic gneiss basement rocks are thrust against, or locally unconformably overlain by, greenschist to lower amphibolite-facies metavolcanic and metasedimentary rocks of probable Archaean to Palaeoproterozoic age (Tingey 1982, 1991, Kovach & Beliatsky 1991). These rocks are overlain by prograde greenschist-facies metasediments.

In northern Prince Charles Mountains (NPCM) geological mapping and detailed petrological and structural studies by SAE and ANARE researchers (Stüwe 1992) recorded widespread felsic gneisses and metasediments, along with minor mafic granulite, intruded by late-tectonic orthopyroxene granitoid (charnockite) bodies. Felsic gneisses were considered by Hensen *et al.* (1992) and Munskgaard *et al.* (1992) to have been derived from *c.* 1800 Ma igneous precursors, possibly formed in a subduction zone environment. They were metamorphosed about 1000 m.y. ago under amphibolite to granulite-facies conditions (Tingey 1991). Five deformations accompanied the granulite-facies event, whereas later deformations occurred under lower-grade, more brittle conditions (Fitzsimons & Thost 1992, Thost & Hensen 1992). Kamenev (1991, 1993) argued that many metamorphic features of both the SPCM and NPCM may be explained in terms of continental collision and crustal thickening, with the two areas having experienced retrograde and prograde metamorphic evolution, respectively. The area between 71° and 73°S is transitional between the two terranes, and is therefore a key area in understanding the geological relationships between the RT and the PMB. Unfortunately, bedrock is relatively poorly exposed, and the area has been little studied.

Fisher Massif (FM), along with mounts Willing and Collins, are the main outcrops in the northern part of this transitional area (Fig. 1). They are characterized by abundant igneous

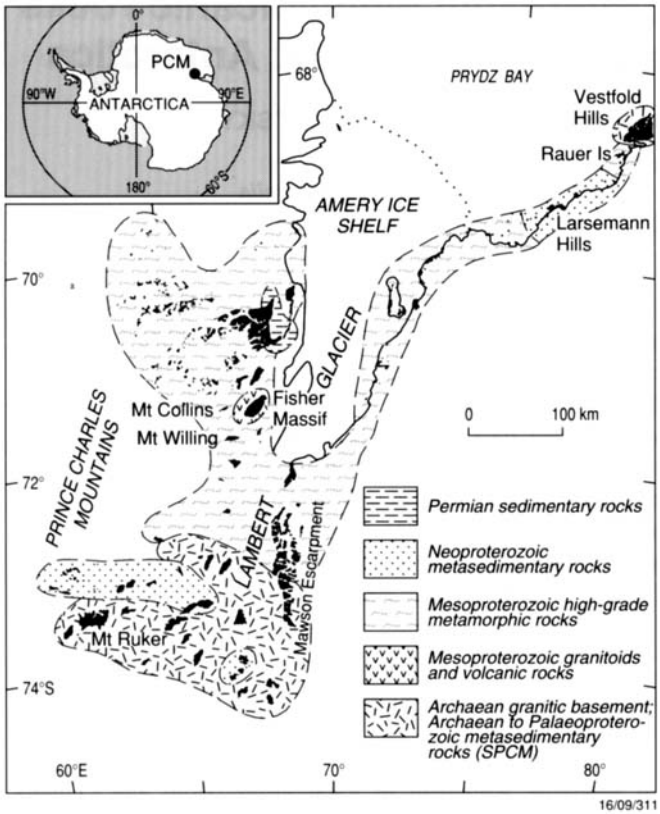

Fig. 1. Generalized geological map of the Prince Charles Mountains–Prydz Bay area (modified from Tingey 1991).

rocks (both volcanic and plutonic) of varied compositions. The geology of FM differs from that of the rest of the NPCM in being of much lower metamorphic grade and having abundant metavolcanic rocks. The proportion of mafic rocks (metabasalt) is much greater than elsewhere in the NPCM, where felsic orthogneiss and subordinate metasediments predominate. However, geochemical data (Sheraton unpublished) suggest that metagabbro and granite at Mount Willing are probably related to some of the FM igneous rocks.

Preliminary U-Pb zircon data show that intermediate and felsic metavolcanic rocks at FM were emplaced about 1300 m.y. ago (Beliatsky *et al.* 1994), consistent with an ion-microprobe U-Pb zircon age of 1283 ± 21 Ma for a metadacite (Kinny *et al.* in press). Isotopic ages of the plutonic rocks are more varied. Ion-microprobe U-Pb zircon ages of 1293 ± 28 Ma for granodiorite and 1020 ± 48 for granite from FM have been obtained (Kinny *et al.* in press), whereas a Rb-Sr whole-rock isochron age of 870 Ma was reported by Krasnikov & Federov (1992). Syenitic and granitic rocks at Mount Collins have both given ion-microprobe emplacement ages of about 980 Ma (Kinny *et al.* in press). Comparisons with the ion-microprobe data suggest that a 1400 Ma conventional U-Pb zircon age reported for one of three syenitic rocks at Mount Collins by Mikhalsky *et al.* (1993) reflects inheritance, and that the emplacement age (or ages) is similar, but may not be identical, to that of Black's sample. Many of the FM granitoids (particularly tonalite and granodiorite) have compositions (marked Y depletion, little Sr depletion) suggesting partial melting of a plagioclase-poor mafic source, so that they apparently represent new felsic crust (Sheraton *et al.* in press). In contrast, the Mount Collins granites have compositions more consistent with melting of felsic crustal rocks.

This paper presents a reconnaissance geochemical study of the metavolcanic rocks designed to elucidate the geological history of FM and provide constraints on its palaeotectonic environment. Geological studies of FM were carried out during three field seasons between 1985 and 1991. Field observations, mostly by A. A. Laiba, provide the geological background for the present study and are summarized below.

Geological outline

Fisher Massif is an isolated, NE–SW orientated, uplifted highland block some 8–12 km wide and 32 km long. It is made up of metavolcanic and minor tuffaceous rocks, clastic metasediments, chert, and ironstone intruded by various plutonic bodies (gabbro, diorite, tonalite, granodiorite, and granite, covered by a moraine veneer some tens of metres thick (Fig. 2). Most of the granitic rocks are of I-type (derived by melting of igneous source rocks), although a small body of S-type (derived by melting of sedimentary rocks) two-mica granite crops out near the centre of FM (Mikhalsky 1993). The volcanic rocks were metamorphosed under lower amphibolite-facies conditions, although their metamorphic history and the peak metamorphic conditions are poorly known. Preliminary petrographical and mineralogical studies suggest metamorphic temperatures between 585 and 640°C, using the garnet-biotite and amphibole-plagioclase geothermometers of Perchuk *et al.* (1985) (N. N. Krasnikov, personal communication 1991). Retrograde greenschist-facies assemblages were developed. Most of the intrusive rocks are also metamorphosed, but biotite±hornblende-bearing granitic rocks have relict igneous hypidiomorphic to allotriomorphic textures and zoned plagioclase phenocrysts occur locally. Rare dykes of metadolerite, dacite, trachydolerite and unmetamorphosed ultramafic rocks are present. Hereafter the prefix 'meta' is omitted from rock names for brevity.

Volcanic rocks are best exposed in a 400 m high escarpment that forms the south-eastern and southern slopes of FM. They mostly dip steeply to the NNW or NW at 50–80°, but more gently (25–50°) in the south-eastern part. Lava flows and tuffaceous beds are commonly 10–20 m thick, and rarely up to 200 m. Field studies have revealed at least four successive sequences of different lithology (Fig. 3). However, thin upper flow zones locally exhibit chilled textures suggesting that the bedding is overturned. Overturning is supported by the fact that the markedly tuffaceous sequence 4 is not intruded by felsic subvolcanic bodies which are characteristic of sequences 1–3 and were presumably intruded prior to, or

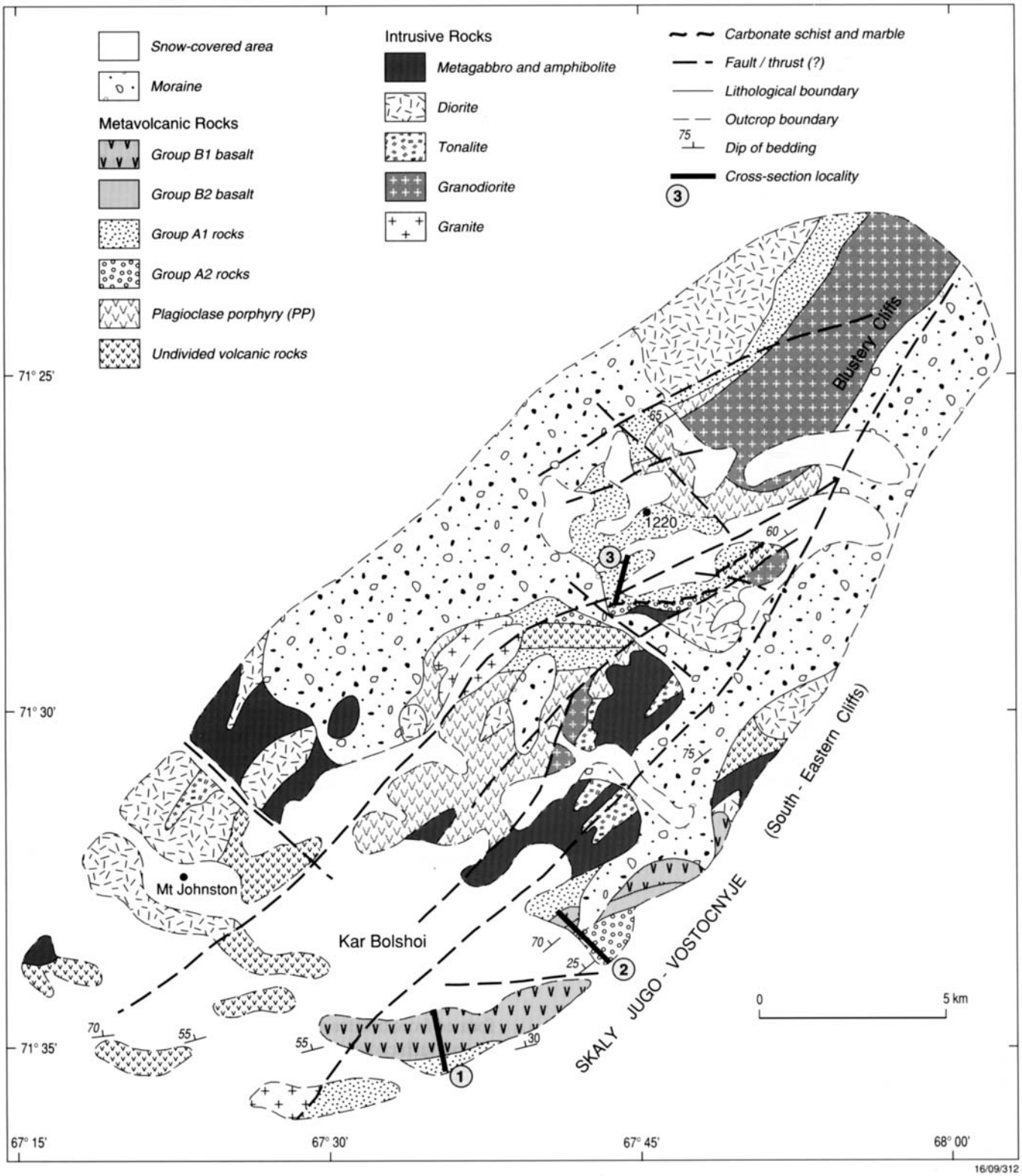

Fig. 2. Geological map of Fisher Massif (modified from Kamenev *et al.* 1993), showing locations of measured sections.

contemporaneously with, the emplacement of sequence 4 rocks. Moreover, chemical data are more consistent with sequence 1 being the oldest (see below). In the following discussion, it is therefore assumed that the volcanic succession is overturned and the various units are described in order of decreasing stratigraphical age.

https://doi.org/10.1017/S0954102096000120 Published online by Cambridge University Press

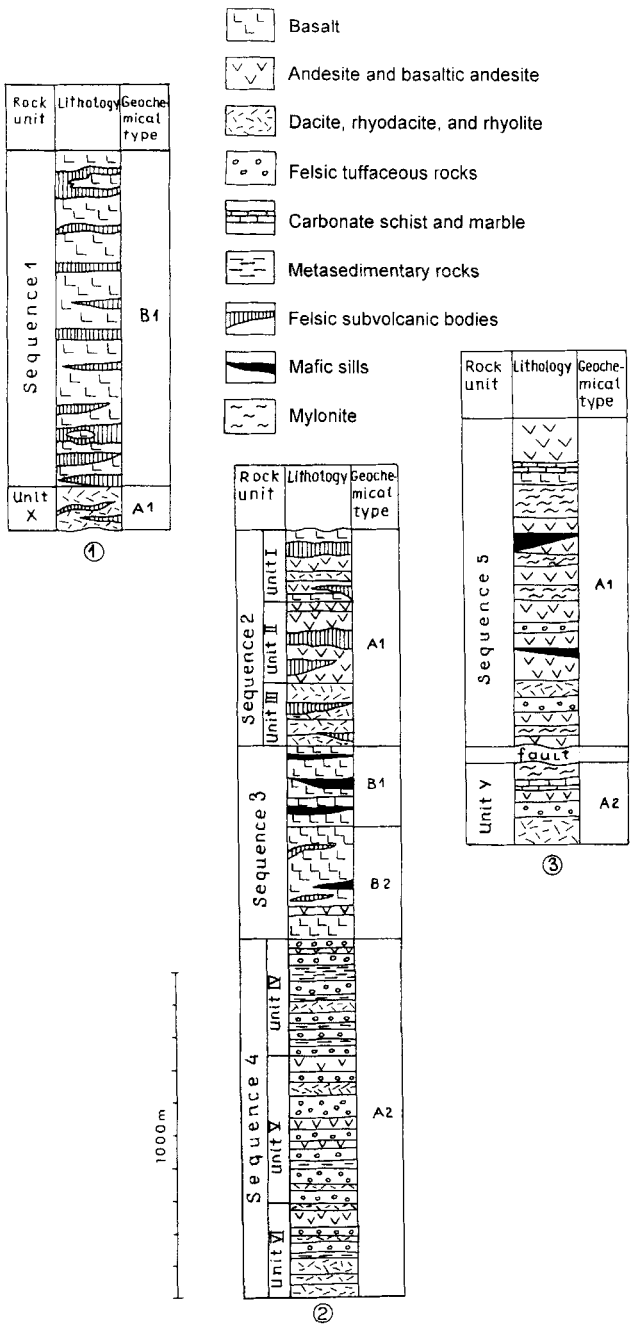

Fig. 3. Schematic measured sections (see Fig. 2 for locations). Note that the sections are depicted as in outcrop, but they are interpreted as having been overturned, with sequence 1 being the oldest.

The presumed oldest sequence (1) is at least 1000 m thick and crops out in the southern part of Kar Bolshoi (Fig. 2). It is composed of fine-grained aphyric or rarely porphyritic basalt, intruded by numerous, mainly felsic subvolcanic bodies (predominantly sills, although dykes, small laccoliths of complex shape, and probable necks are also present). Porphyritic basalt forms thin layers and beds (0.2–3.0 m) and contains up to 25% of plagioclase megacrysts which are probably of cumulate origin. Subvolcanic bodies, which vary greatly in size (0.5–100 m), form 50% of the sequence. They consist of dacite and rhyodacite, with minor andesite, and contain numerous basaltic xenoliths. Porphyritic textures are common and there are abundant quartz megacrysts. Near the base of the escarpment, sequence 1 rocks are overlain by a 130 m thick unit of dacite (unit X), also intruded by felsic subvolcanic bodies.

The 650 m thick sequence 2, exposed in the north-eastern flank of Kar Bolshoi, consists of basalt (3%), basaltic andesite (40%), andesite (27%) and dacite (30%), intruded by numerous intermediate to felsic subvolcanic bodies which form a total of 200 m of section. Lithological and textural features enable sequence 2 to be subdivided into three units (I–III; Fig. 3). Unit I comprises aphyric basalt, basaltic andesite, andesite, and dacite. Unit II consists of intercalated beds of basaltic andesite and andesite. Unit III is composed mostly of dacite and rhyodacite, with the latter predominating higher in the section. Felsic subvolcanic bodies intrude all three units. None of units I–III may be directly correlated with unit X, but similar dacitic compositions allow a tentative correlation of the latter with the lowermost part of sequence 2, from which it is separated by an east-west trending fault.

Sequence 3 (600 m thick) overlies unit III and is composed mainly of massive or slightly schistose, locally diffusely layered, aphyric basalt, with one 2 m thick plagioclase-phyric flow. There are also minor (5–10%) amounts of other rock types, including felsic subvolcanic rocks. Concordant bodies, 6–27 m thick, of mafic rock with coarse-grained, relict ophitic or gabbroic textures in the lower part of the section are probably sills. In the upper part of the section, schistose aphyric fine-grained basalt, commonly exhibiting cataclastic structures, predominates. Some relatively melanocratic beds consist of amphibolite.

Sequence 4 (1100 m) is composed of volcanic (23%) and tuffaceous (62%) rocks, and schistose metasediments (15%). Volcanic rocks comprise basaltic andesite (27%), andesite (25%), dacite (24%), and rhyodacite (24%). Three lithological units (IV, V, VI) are distinguished (Fig. 3). Unit IV consists of tuffaceous fine or coarse-grained lapilli(?)-bearing rocks of andesitic to dacitic composition, intercalated with 1–50 m thick beds of fine-grained micaceous quartz-feldspar schist formed from tuffites and/or silty sandstones. Unit V is made up of tuffaceous rocks of andesite to basaltic andesite composition, which range widely in grain size; some beds contain abundant lapilli(?) and/or volcanic bombs (0.1–0.5 m) in sheared isometric blocks and lenses. There are also rare beds and layers of andesite, dacite and possible metasedimentary rocks. Unit VI comprises thin (0.3–3 m) intercalated units of andesite, dacite, rhyodacite, and fine-grained banded tuff. As a whole, sequence 4 does not show a consistent trend towards more felsic rocks, but rather a number of andesite-dacite cycles. As already pointed out, the felsic subvolcanic bodies which are common in sequences 1–3 are absent from sequence 4.

https://doi.org/10.1017/S0954102096000120 Published online by Cambridge University Press

Somewhat different rock types occupy the central and northern parts of FM. The southern and western slopes of the 1220 m high peak (Fig. 2) are made up of a poorly exposed 1000 m thick succession (sequence 5) of light-coloured globular fine-grained andesite and minor basaltic andesite and dacite in beds some tens of metres thick. Locally these rocks are mylonitized. A few 10–20 m thick conformable layers of marble and carbonate schist are intensely deformed and recrystallized, and probably mark thrust zones. Sequence 5 may be roughly correlated with sequence 2 on the basis of bulk rock compositions, although detailed correlations at unit scale are not possible. Sequence 5 is ovelain by a 200–300 m thick sequence of dacite, tuffaceous rocks of andesitic to dacitic composition, and minor carbonate rocks (unit Y), but the contact is obscured by scree and may be of fault (thrust?) origin. The northern and eastern slopes of the same peak are made up predominantly of dark-coloured basaltic andesite containing sparse (up to 5%) plagioclase megacrysts (probably phenocrysts), but lacking globular structures. These rocks are hereafter referred to as plagioclase porphyries (PP). In a few localities they contain large andesite and marble blocks, which implies that PP may at least partly be intruded into sequence 5 rocks.

The structure of FM appears to be dominated by a number of tectonic blocks and/or nappes. However, no regional faults or thrusts have been found within the 1500 m thick sequences 2–4, which are therefore considered to represent an actual succession of volcanic flows making up a thick tectonic slab or nappe. The total thickness of the rocks studied exceeds 2600 m (or 3300 m including subvolcanic bodies intruded into sequences 1–3), basaltic rocks being the most abundant (Fig. 4).

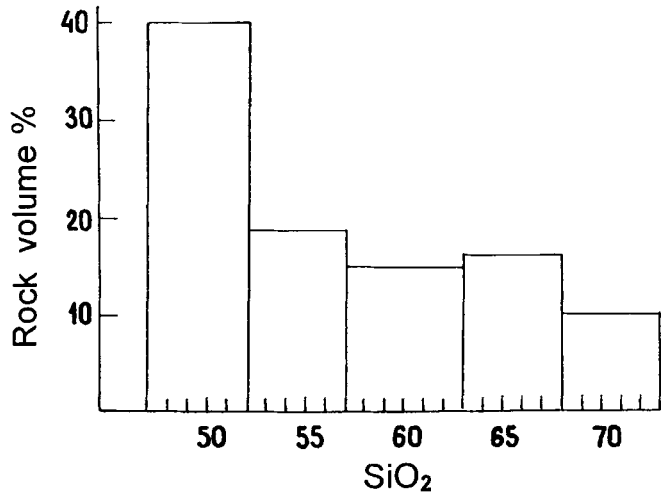

Fig. 4. Histogram of SiO_2 contents. Subdivisions correspond to the SiO_2 contents of basalt, basaltic andesite, andesite, dacite, and rhyolite of Le Maitre's (1989) classification of volcanic rocks.

Petrography

Metamorphosed basalt and basaltic andesite are dark greenish-grey fine-grained rocks with a characteristic pervasive schistosity, although massive varieties also occur. Most rocks are aphyric or contain rare recrystallized plagioclase megacrysts up to 1 cm long, but abundant plagioclase megacrysts (10–25% of rock volume) occur in some cumulate rocks. Metamorphic nematoblastic, porphyroblastic, and blastocataclastic textures predominate, but relict intersertal, microlitic, and locally ophitic textures are distinguishable in the groundmass. The latter consists mostly of small plagioclase (oligoclase-andesine) laths and isometric grains (10–50%) and subparallel fine prismatic grains or porphyroblasts of hornblende and actinolite. Minor minerals are biotite, quartz, epidote, chlorite, opaque minerals, sphene, carbonate, sericite, and garnet. Colour index ranges widely between 40 and 90, with the most mafic varieties being coarse-grained amphibolite. Globular structures of secondary quartz are common. PP are fine to coarse-grained and commonly exhibit relict ophitic textures. They are similar to other mafic rocks except for higher phenocryst abundances (up to 5%) and a lack of globular structures; their colour index ranges from 45 to 50.

Meta-andesites are grey, fine-grained, schistose to diffusely layered or homogeneous rocks, with colour indices between 20 and 35. They are commonly porphyritic, but lepidoblastic, nematogranoblastic, and cataclastic textures predominate. Sparse zoned plagioclase megacrysts (up to 2 mm) are enclosed in a relict felsitic or prismatic matrix, and a few rocks contain deformed K-feldspar megacrysts. Mafic minerals comprise amphibole (bluish-green hornblende, secondary actinolite, and rare cummingtonite; up to 35%), biotite (up to 25%), epidote (up to 10%) and opaque minerals (2–7%), and small amounts of chlorite, garnet, carbonate and sericite may also be present. Hornblende forms porphyroblasts up to 3 mm long in some rocks. Andesites of sequence 4 are typically biotite rich, whereas most of those in other sequences are amphibole rich.

Dacite and rhyodacite are light-coloured, sparsely porphyritic, massive or schistose rocks with up to 5% of phenocrysts. Metamorphic porphyroblastic, lepidoblastic, and blastocataclastic textures are common. Relict phenocrysts comprise quartz, K-feldspar, and recrystallized plagioclase (0.5–1.5 mm) grains or glomeroporphyritic segregations. The felsitic groundmass (quartz and feldspar) contains various amounts of bluish hornblende, pale green actinolite, epidote, colourless cummingtonite, and biotite. Common minor phases are sericite, opaque minerals, garnet, chlorite, calcite, sphene, apatite, and zircon. Colour index ranges from 10 to 25.

Variously coloured fine- to coarse-grained schistose tuffaceous rocks commonly exhibit thin compositional layering and contain finer-grained felsic inclusions up to 1 cm across, interpreted as lapilli. The matrix consists of fine-grained aggregates of quartz and feldspar. Some beds

Table I. Representative chemical analyses of volcanic and subvolcanic rocks from Fisher Massif.

Sample	1 39712-4	2 36712-17	3 36712-18	4 36717-4	5 36811-13	6 36811-19	7 334	8 31030-2	9 34521-7
SiO_2	49.04	50.57	50.44	47.72	48.50	50.64	52.30	49.90	53.78
TiO_2	1.02	0.93	1.07	1.01	0.97	1.54	1.11	1.21	0.73
Al_2O_3	14.84	15.50	13.87	16.45	14.50	15.18	18.05	19.00	16.79
Fe_2O_3	2.32	1.89	2.46	2.24	2.44	2.55	2.18	2.87	3.10
FeO	9.01	7.58	9.20	7.25	9.22	8.99	7.63	7.11	6.24
MnO	0.20	0.14	0.17	0.13	0.19	0.17	0.12	0.18	0.13
MgO	8.64	7.22	6.97	6.73	8.01	6.25	3.00	4.50	4.96
CaO	10.30	11.68	11.41	12.34	11.31	8.52	8.59	8.91	9.46
Na_2O	2.19	2.77	2.18	2.11	2.14	3.27	3.50	4.06	1.78
K_2O	0.12	0.12	0.17	0.72	0.15	0.25	1.50	0.67	1.05
P_2O_5	0.08	0.11	0.11	0.10	0.07	0.20	0.32	0.22	0.20
LOI	2.24	1.47	1.93	3.20	2.48	2.42	1.44	1.43	1.77
Total	100.01	99.98	99.97	99.99	99.99	99.97	99.74	100.06	99.98
Trace elements in parts per million									
Ba	34	61	50	163	50	97	322	195	391
Rb	1	1	<1	15	2	5	30	12	26
Sr	171	170	182	164	127	177	436	376	614
Pb	5	<2	<2	4	2	5	nd	nd	4
Th	<2	<2	<2	<2	<2	5	5	10	<2
U	<0.5	<0.5	<0.5	0.5	<0.5	2.5	nd	nd	1.0
Y	26	25	30	26	29	35	23	20	11
Zr	70	75	74	73	59	118	97	77	51
Hf	<2	<2	<2	<2	3	4	nd	nd	2
Nb	3	4	3	<2	<2	12	7	8	<2
La	2	3	3	<2	3	5	nd	nd	6
Ce	13	12	14	6	7	21	nd	nd	23
Nd	5	7	4	5	5	15	nd	nd	13
Sc	55	46	51	45	60	40	nd	nd	38
Cr	302	240	127	222	123	45	18	59	86
Ni	74	79	52	90	59	56	8	25	25
Co	nd	nd	nd	nd	nd	nd	27	34	nd
V	284	248	306	274	330	259	234	288	381
Ga	16	16	17	15	17	18	nd	nd	20
mg	63.5	63.4	57.6	61.8	61.0	55.2	41.1	50.8	55.0
Zr/Nb	23	19	25	-	-	9.8	14	9.6	-
Zr/Y	2.7	3.0	2.5	2.8	2.0	3.3	4.2	3.9	4.6
Zr/Rb	70	75	-	4.8	30	24	3.2	6.4	2.0
K/Ba	29	16	28	37	25	21	38.7	28.5	22.3
K/Rb	1000	1000	-	400	620	420	415	460	335
Ba/Zr	0.48	0.81	0.67	2.23	0.85	0.82	3.3	2.5	7.6
Ti/Zr	87	74	87	83	99	78	68	94	86
P/Zr	5.0	6.4	6.5	6.0	5.2	7.4	14	12	17
Rb/Sr	0.006	0.006	-	0.091	0.016	0.028	0.069	0.032	0.042
La/Ce	0.15	0.25	0.21	-	0.43	0.24	-	-	0.26
Y/Nb	8.6	6.3	10	-	-	2.9	3.3	2.5	-
La/Nb	0.7	0.8	1	-	-	0.4	-	-	-
Ba/La	17	20	17	-	17	19	-	-	65
$(Ce/Y)_N$	1.25	1.20	1.17	0.58	0.60	1.50	-	-	5.2

LOI = Loss on ignition, nd = not determined, mg = atomic $100Mg/(Mg + 0.8Fe_{total})$, $(Ce/Y)_N$ = chondrite-normalized. 1–5 = Group B1 basalts; 6 = Group B2 basalt; 7–10 = Plagioclase porphyries (PP); 11–17 = Group A1 rocks: 11–12 = Basaltic andesites (sequence 2), 13 = Andesite (sequence 2), 14–16 = Basaltic andesites (sequence 5), 17 = Dacite (sequence 5); 18–24 = Group A2 rocks: 18 = Dacite (unit Y), 19–21 = Andesites (sequence 4), 22 = Rhyodacite (sequence 4), 23–24 = Rhyolites (sequence 4); 25–27 = Rocks from subvolcanic bodies: 25 = Andesite, 26–27 = Rhyolites.

https://doi.org/10.1017/S0954102096000120 Published online by Cambridge University Press

Table I. Cont.

Sample	10 34521-12	11 36812-6	12 36812-14	13 36812-20	14 31026-1	15 34518-12	16 34518-14	17 34518-2	18 34516-1
SiO_2	55.50	54.03	54.95	61.01	54.30	53.57	53.75	63.73	65.01
TiO_2	0.97	1.17	0.96	0.74	0.64	1.10	1.18	0.54	0.50
Al_2O_3	17.54	14.55	18.10	14.21	14.50	13.90	14.25	14.25	15.50
Fe_2O_3	3.11	3.72	2.43	2.24	2.86	2.74	2.86	2.27	1.73
FeO	5.36	5.66	6.16	4.95	7.37	7.26	7.19	3.17	3.22
MnO	0.13	0.12	0.12	0.13	0.14	0.23	0.20	0.13	0.13
MgO	2.80	3.54	3.28	3.82	8.41	6.62	5.34	2.84	2.94
CaO	8.97	8.33	5.94	5.97	4.12	9.42	8.02	6.29	3.66
Na_2O	2.68	3.35	4.17	2.99	1.90	2.42	4.11	3.79	4.54
K_2O	0.84	0.83	1.26	1.29	2.00	0.36	0.24	0.39	1.13
P_2O_5	0.30	0.22	0.83	0.18	0.03	0.29	0.25	0.10	0.18
LOI	1.77	3.99	1.80	2.36	2.43	1.72	1.99	2.30	1.26
Total	99.97	99.51	100.00	99.88	99.90	99.13	99.38	99.29	100.12
Trace elements in parts per million									
Ba	242	252	362	458	376	15	92	3	452
Rb	16	26	26	35	104	18	24	22	20
Sr	744	294	311	455	130	328	420	324	198
Pb	7	4	4	7	nd	nd	nd	nd	nd
Th	<2	2	4	6	<2	10	<2	1	3
U	<0.5	<0.5	1.0	<0.5	nd	nd	nd	nd	nd
Y	16	28	28	25	11	15	18	23	31
Zr	75	97	82	120	63	100	118	143	181
Hf	3	2	<2	4	nd	nd	nd	nd	nd
Nb	4	4	7	9	8	10	7	11	6
La	13	9	24	20	nd	nd	nd	nd	nd
Ce	31	25	49	45	nd	nd	nd	nd	nd
Nd	16	11	24	22	nd	nd	nd	nd	nd
Sc	34	35	27	24	nd	nd	nd	nd	nd
Cr	25	24	5	125	160	315	158	123	59
Ni	10	14	4	47	31	41	29	43	21
Co	nd	nd	nd	nd	42	34	39	17	21
V	392	317	209	168	208	220	293	120	103
Ga	20	17	19	16	nd	nd	nd	nd	nd
mg	43.3	46.7	46.7	55.0	65.3	60.3	54.9	54.8	57.8
Zr/Nb	19	24	12	13	7.9	10	17	13	30
Zr/Y	4.7	3.4	2.9	4.8	5.7	6.6	6.6	6.2	5.8
Zr/Rb	4.7	3.7	3.1	3.4	0.61	5.5	4.9	6.5	9.1
K/Ba	28.8	27.3	28.9	23.3	44.2	200	21.7	1100	20.8
K/Rb	440	265	400	306	159	170	83	150	470
Ba/Zr	3.2	2.6	4.4	3.8	5.9	0.15	0.77	0.02	2.5
Ti/Zr	78	72	70	37	61	66	60	23	17
P/Zr	17	9.9	44	6.6	2.1	13	9.3	3.1	4.3
Rb/Sr	0.022	0.088	0.084	0.077	0.80	0.055	0.057	0.67	0.10
La/Ce	0.42	0.36	0.48	0.44	-	-	-	-	-
Y/Nb	4.0	7.0	4.0	2.8	1.4	1.5	2.6	2.1	5.2
La/Nb	3.3	2.3	3.4	2.2	-	-	-	-	-
Ba/La	19	28	15	23	-	-	-	-	-
$(Ce/Y)_N$	4.8	2.2	4.4	4.5	-	-	-	-	-

also contain up to 20% of large bombs (up to 50 cm across) of dacitic or rhyodacitic composition. The colour index ranges from 15 to 40, with biotite, bluish hornblende, actinolite, epidote, and opaque minerals being common mafic phases.

Minor beds of fine-grained light-coloured micaceous (mostly muscovite-bearing) plagioclase-quartz schist contain small amounts of epidote, garnet, apatite, and tourmaline. Colour index ranges between 10 and 30. They probably represent metamorphosed immature tuffaceous sandstones, silty sandstones, or tuffites.

Dacitic to rhyolitic subvolcanic bodies are relatively massive

https://doi.org/10.1017/S0954102096000120 Published online by Cambridge University Press

Table I. Representative chemical analyses of volcanic and subvolcanic rocks from Fisher Massif. (Cont.)

Sample	19 36719 -16	20 36719 -24	21 36719 -17	22 36719 -26	23 36720 -1	24 36726 -17	25 36712 -7	26 36712 -23	27 36712 -25
SiO_2	56.83	59.70	61.74	69.77	72.35	73.44	61.26	70.90	73.83
TiO_2	0.66	0.64	0.59	0.48	0.42	0.41	0.45	0.24	0.28
Al_2O_3	15.42	14.61	15.22	13.32	12.90	12.70	14.47	13.36	12.97
Fe_2O_3	2.58	3.83	3.04	1.75	1.97	1.27	0.75	1.53	1.38
FeO	5.30	5.55	4.76	3.09	1.84	1.91	8.91	2.55	2.05
MnO	0.10	0.17	0.09	0.12	0.09	0.08	0.10	0.08	0.07
MgO	4.44	3.47	2.84	1.24	0.79	0.72	4.70	1.30	1.06
CaO	6.18	4.58	3.57	2.75	3.91	3.47	4.45	4.84	2.52
Na_2O	3.58	1.89	3.41	3.30	2.02	2.35	3.06	3.36	4.01
K_2O	2.39	3.01	2.55	1.96	2.28	1.60	0.05	0.26	0.54
P_2O_5	0.26	0.17	0.16	0.13	0.08	0.06	0.08	0.05	0.07
LOI	2.26	2.33	2.03	2.08	1.36	1.94	1.72	1.52	1.16
Total	100.00	99.95	100.00	99.99	100.01	99.95	99.99	99.99	99.94
Trace elements in parts per million									
Ba	733	494	1187	1082	1324	915	51	80	154
Rb	48	75	61	47	54	41	<1	4	10
Sr	699	432	726	391	298	385	355	241	128
Pb	11	10	11	12	9	13	4	<2	2
Th	8	3	8	8	9	9	3	<2	2
U	1.0	1.0	0.5	<0.5	3.0	1.0	1.5	1.0	<0.5
Y	19	22	18	26	34	33	21	12	19
Zr	115	58	90	107	152	164	87	63	93
Hf	4	<2	3	4	4	6	3	<2	3
Nb	5	3	3	3	4	5	5	5	3
La	26	13	12	25	31	32	5	<2	5
Ce	52	35	36	57	64	72	15	10	16
Nd	25	18	14	27	32	33	8	3	4
Sc	24	25	21	15	13	12	23	16	14
Cr	113	65	73	10	9	6	55	29	5
Ni	43	16	32	3	2	3	25	7	2
Co	nd	nd	nd	nd	nd	nd	nd	nd	nd
V	318	243	190	57	35	20	132	71	28
Ga	18	16	18	15	14	14	20	15	11
mg	56.5	46.2	45.8	37.2	32.8	34.4	52.2	42.4	41.8
Zr/Nb	23	19	30	36	38	33	17	13	31
Zr/Y	6.1	2.6	5.0	4.1	4.5	5.0	4.1	5.3	4.9
Zr/Rb	2.4	0.77	1.4	2.3	2.8	4.0	-	16	9.3
K/Ba	27.1	50.6	17.8	15.0	14.3	14.5	8.1	27	29
K/Rb	413	333	347	346	350	323	-	540	450
Ba/Zr	6.4	8.5	13.2	10.1	8.7	5.6	0.58	1.27	1.65
Ti/Zr	34	66	39	27	17	15	31	23	18
P/Zr	9.9	13	7.8	5.3	2.3	1.6	4.0	3.5	3.3
Rb/Sr	0.068	0.17	0.084	0.120	0.181	0.106	-	0.017	0.078
La/Ce	0.50	0.37	0.33	0.48	0.48	0.44	0.33	-	0.31
Y/Nb	3.8	7.3	6.0	8.6	8.5	6.6	4.2	2.4	6.3
La/Nb	5.2	4.3	4	8	8	6	1.0	-	1.6
Ba/La	28	38	99	43	43	29	10	-	31
$(Ce/Y)_N$	6.8	4.0	5.0	5.5	4.7	5.5	1.8	2.1	2.1

and coarse grained (0.5–1 mm), with colour indices between 10 and 35. They contain abundant (10–20%) zoned plagioclase and, in some rocks, quartz phenocrysts, quartz globules (amygdales?), and various amounts of prismatic amphibole, biotite, chlorite, carbonate, sericite, opaque minerals, and apatite.

Geochemistry

Major elements

Eighty samples of metavolcanic rocks (including subvolcanic and tuffaceous rocks) were analysed at AGSO by X-ray fluorescence spectrometry (XRF) (Norrish & Hutton 1969)

https://doi.org/10.1017/S0954102096000120 Published online by Cambridge University Press

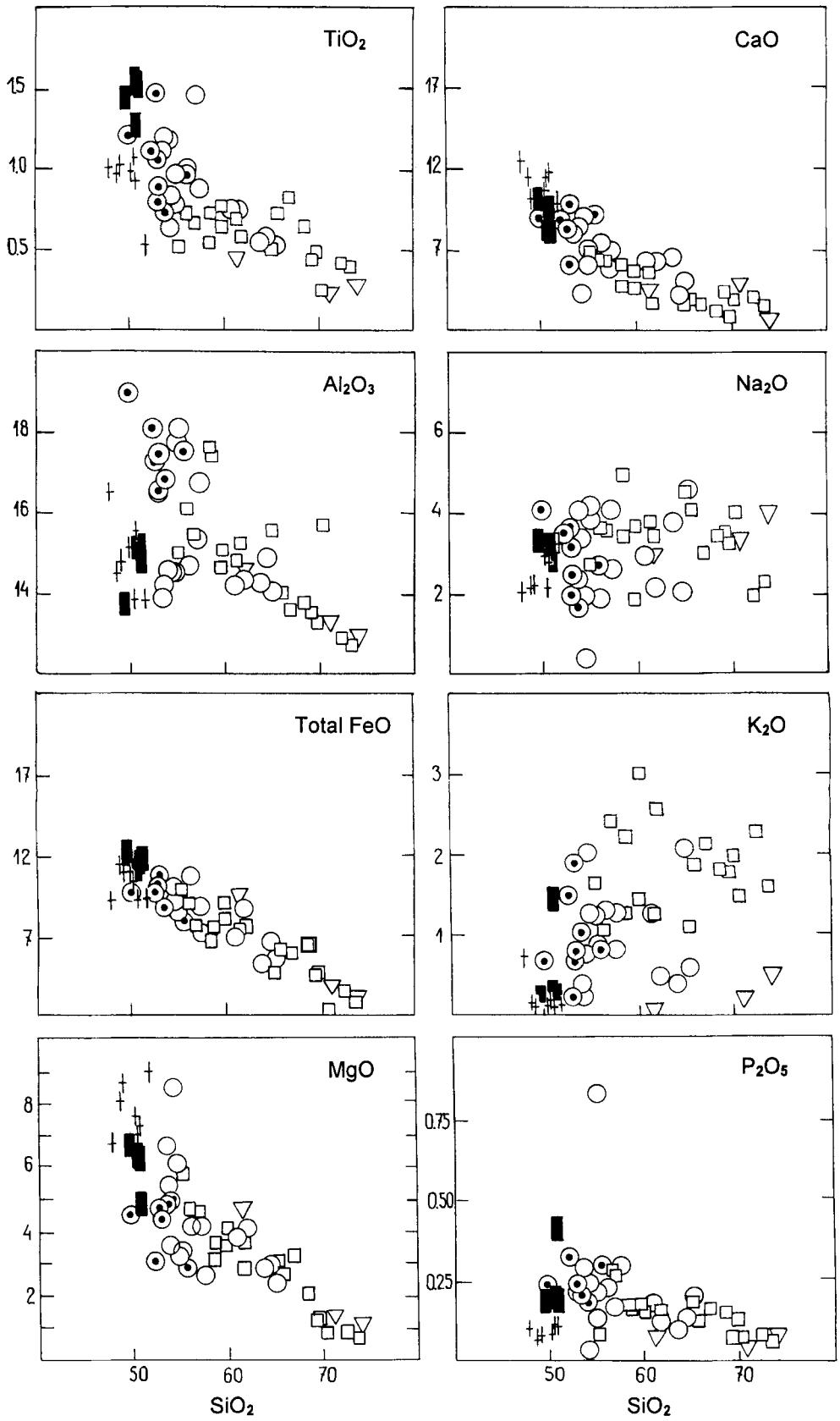

Fig. 5. SiO_2 variation diagrams. † = group B1 basalts, ■ = group B2 basalts, ⊙ = plagioclase porphyries, ○ = group A1 rocks, □ = group A2 rocks, ∇ = subvolcanic rocks.

https://doi.org/10.1017/S0954102096000120 Published online by Cambridge University Press

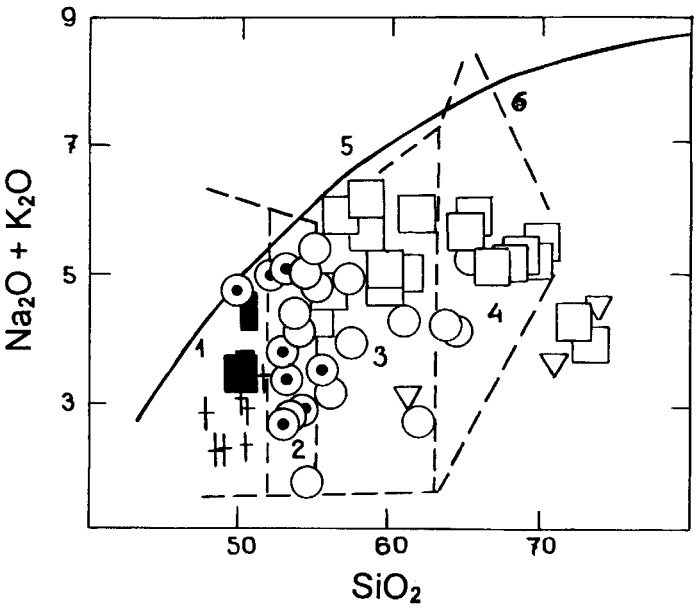

Fig. 6. SiO_2 - (Na_2O+K_2O) plot. Dividing line between alkalic (upper) and sub-alkalic fields from Miyashiro (1978). (1) Basalt, (2) basaltic andesite, (3) andesite, (4) dacite, (5) trachyandesite, and (6) rhyolite fields after Cox *et al.* (1979). Symbols as in Fig. 5.

or at PMGRE by wet chemistry. Samples analysed at both laboratories show good agreement, and therefore both sets of data are plotted on the variation diagrams. Representative analyses are listed in Table 1.

Fisher Massif metavolcanic rocks show wide and continuous variation trends for SiO_2 (47–74%), MgO (1–9%), and other major elements, without any significant compositional gaps (Figs 4 & 5). The plots demonstrate negative correlations between SiO_2 and FeO_{total}, MgO, CaO, Al_2O_3, and TiO_2, suggesting that fractionation processes strongly modified the primary melt compositions. All samples plot within the sub-alkaline field on Fig. 6, but show a wide range of alkali contents, even within individual rock groups. Such wide variations, together with extremely low alkali contents in some samples, suggest redistribution during late-magmatic or, more likely, subsequent (metamorphic) processes. However, consistently low K_2O in the subvolcanic rocks may be a primary feature.

Some of the volcanic sequences distinguished in the field have distinctive major element compositions, although there is some overlap. Basalts in the upper part of sequence 3 differ from other basalts in having higher TiO_2, P_2O_5, Na_2O, and K_2O, but lower MgO and CaO contents and *mg* values (*mg* = atomic 100Mg/(Mg+0.8Fe_{total}) = 47–55). They are slightly Q-normative tholeiites, and are termed B2 basalts. Other basalts (sequence 1 and the rest of sequence 3) have higher *mg* (55–67) and are slightly Ol-normative tholeiites, hereafter referred to as B1 basalts.

Plagioclase porphyries (PP) have characteristically high Al_2O_3 contents (16.5–19.0%), with most samples plotting within the basaltic andesite field (Fig. 6); *mg* ranges widely from 39 to 55. Most major elements do not show clearly defined trends on SiO_2 or *mg* variation diagrams. The variations in alkali contents are too large to be due to fractionation or different degrees of partial melting and probably reflect secondary alteration. On an alkali index (AI) - Al_2O_3 plot (Fig. 7), PP samples plot apart from other basalts and basaltic andesites, straddling the dividing line between high-alumina and tholeiitic basalts.

Andesites, dacites, and rhyodacites of sequences 2 and 5 have wide ranges of silica contents (53–65%), TiO_2, FeO_{total}, MgO, CaO, and, in particular, K_2O and Na_2O (Fig. 5). One sample has unusually high MgO (8.41%) and may be a cumulate, whereas another has very high P_2O_5 (0.83%). *mg* ranges from 45 to 65. These rocks are defined as group A1.

Sequence 4 rocks have an even wider range of composition, from andesite to rhyolite (SiO_2 = 55–73%), and tend to have higher K_2O contents than those of sequences 2 and 5. The andesitic rocks have particularly high K_2O (2.39–3.01%), being of high-K type using the classification of Le Maitre (1989), whereas the more felsic rocks are mostly of medium-K type. Dacites of unit Y, in the northern part of FM, also have relatively high K_2O and are classified with sequence 4 as group A2. These rocks have low Alumina Saturation Index values (ASI = molecular Al_2O_3/(CaO+Na_2O+K_2O), after White & Chappell 1983), ranging from 0.85 to 1.03, with a few rocks up to 1.10; they are thus of I-type, that is, derived by melting of igneous source rocks.

Thin subvolcanic bodies of andesite, dacite and rhyodacite cutting sequences 1–3 have major element compositions generally similar to rocks of group A2, except that K_2O is much lower.

Trace elements

Twenty samples were analysed for trace elements by XRF at AGSO and another 15 samples (for a smaller range of elements) by XRF at the Institute of Precambrian Geology and Geochronology (IPGG), St Petersburg, using methods similar to those described by Norrish & Chappell (1977). Comparisons between data from the two laboratories show very good agreement, apart from Cr and Ni for which analyses at IPGG are slightly higher. Trace element abundances are particularly useful for comparing different igneous suites and are capable of revealing some of the chemical characteristics of the source as well as the subsequent melt evolution.

Basaltic rocks of group B1 are characterized by low Rb and, in some cases, Nb, La, Ce, and Nd, which is reflected by marked troughs on a primordial mantle (PM)-normalized spidergram (Fig. 8a). Apart from Th (which is below the detection limit of 2 ppm and is plotted as half this value), and Rb (which is strongly depleted in many rocks), most samples show relatively smooth patterns, including many elements (Ba, K, and Sr) commonly mobilized by hydrous fluids. This

implies that, at least for less mobile elements, there are not likely to have been major chemical changes during subsequent metamorphic events. Nevertheless, the Rb and, in some rocks, LREE (light rare-earth element) depletions are probably at least partly secondary features. Much of the scatter for LREE may be due to analytical uncertainties for concentrations which are near to XRF detection limits. Group B1 rocks show broadly similar patterns to N-MORB (Fig. 9a), but somewhat depleted in Nd, P, Ti, and Y, and markedly enriched in LILE (large-ion lithophile elements: Rb, Ba, K, Th, and U). They differ markedly from P-MORB in having lower K, Rb, LREE, and HFSE (high field strength elements: Nb, P, and Zr). Sample 36717–4 differs from the other B1 rocks in being enriched in K, Rb and Ba. Although it also has slightly higher Al_2O_3 and K_2O, thus bearing some compositional resemblance to the PP group, it does not have the high Sr of the latter (Fig. 8e), so that the high LILE are probably due to alteration. B1 basalts are characterized by low (relative to PM) Rb/Sr (0.005–0.006) and Ti/Zr (74–99), similar to high Y/Nb (6–13), and high Zr/Nb (19–24) and Ba/La (17–20) ratios (Table I).

Group B2 basalt 36811–19 is more enriched than B1 basalts for the whole range of incompatible elements (LILE, particularly Th and U, HFSE and LREE), except Sr (Fig. 8b), and has lower Cr (43 ppm) and slightly lower Ni (56 ppm) contents. Other B2 samples, for which only major element data are available, have similar relatively high TiO_2 and P_2O_5 and low MgO (Fig. 5). The N-MORB-normalized spidergram (Fig. 9a) shows consistent enrichment in all trace elements, comparable to P-MORB (or even ocean island basalt, OIB), albeit with slightly different HFSE and LREE abundances and marked, probably secondary, Th and U enrichment. Thus, group B2 shows no Nb or LREE anomalies and differs from group B1 in having higher Rb/Sr (0.028) and lower Zr/Nb (10) and Y/Nb (2.9) ratios.

Basaltic andesites of group PP differ from B1 and B2 basalts in being strongly evolved (Q-normative), depleted in Ti and Y, and having prominent negative Nb and positive Sr anomalies (Figs 8e, 9b); they are more enriched in most LILE. Many incompatible element ratios are quite different to those of group B1 basalts, e.g. higher Zr/Y, K/Zr, Rb/Sr, La/Nb and Ce/Y, and lower K/Rb and Y/Nb.

Rocks of group A1 are enriched in most LILE and LREE, but have similar HFSE contents to B1 and B2 basalts. PM-normalized spidergrams (Fig. 8c) are generally similar to those of the PP group, except for higher HFSE (particularly Ti and Y). A1 rocks have marked negative Nb anomalies, but generally small Sr anomalies. The more siliceous andesite (36812–20) has a small positive Sr anomaly and higher *mg* than the basaltic andesites, clearly inconsistent with fractionation of the latter. However, negative Ti and P anomalies do suggest more extensive fractionation. A2 andesites have generally similar spidergram patterns to group A1 rocks, but tend to be even more LILE-enriched, whereas the rhyodacites and rhyolites have very irregular

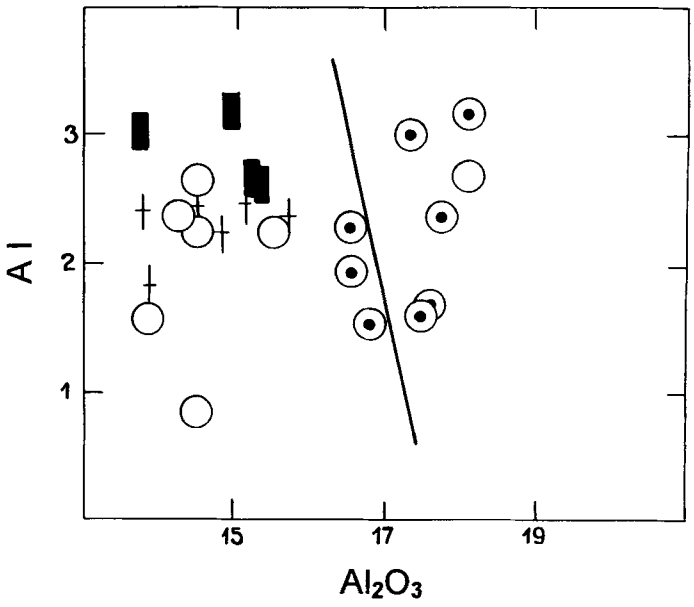

Fig. 7. Alkali Index (AI) - Al_2O_3 plot (after Middlemost 1975). AI= $(Na_2O+K_2O)/[(SiO_2-43)*0.17]$(wt. %). Solid line divides tholeiitic basalt (left) and high-alumina basalt fields. Symbols as in Fig. 5.

patterns with negative Nb, Sr, P, and Ti anomalies (Fig. 8d), typical of felsic igneous rocks in general (Tarney *et al.* 1987). The predominantly felsic subvolcanic rocks differ from the groups A1 and A2 extrusives in their consistently very low LILE and LREE contents, although this may partly be attributable to alteration (andesite 36712–7 has particularly low K_2O, Rb, and La: Fig. 8f).

Isotopic data

Three metavolcanic and three granodiorite samples from FM were analysed for Rb, Sr, Sm, and Nd isotopes at IPGG. The latter rocks were included to investigate possible genetic relationships to the extrusive rocks. A cation-exchange technique was used to extract these elements, and isotopic abundances were determined by the isotope dilution method, using a Finnigan MAT-261 8-collector mass spectrometer. Isotopic data are presented in Table II.

Sample 31026–1 (a basaltic andesite of group A1) is highly Rb-enriched and Sr-depleted compared to other A1 rocks, suggesting either that it belongs to a distinct suite, or that there was some redistribution of Rb and Sr during subsequent thermal events. As this sample falls far outside the range of Rb and Sr contents of other A1 and A2 andesites and has an unrealistically low Sri value (0.686), the latter seems most plausible. Assuming the metavolcanic rocks to be 1300 m.y. old (Beliatsky *et al.* 1994), the initial $^{87}Sr/^{86}Sr$ ratio for sample 31030–2 (plagioclase porphyry) is 0.7035 and for sample 34516–1 (group A2 dacite) 0.7041. Calculated initial $^{143}Nd/^{144}Nd$ (T = 1300 Ma) ratios for metavolcanic rocks range from 0.51104 to 0.51109, with $\varepsilon^{1300}Nd$ from +1.6

https://doi.org/10.1017/S0954102096000120 Published online by Cambridge University Press

to +2.5. The granodiorites have somewhat higher ε^{1300}Nd values (+2.4 to +3.0), but the difference only slightly exceeds the analytical uncertainty (±0.5 ε). Nd_{DM} model ages are 1870–2250 and 1640–1700 Ma, respectively, although the former are of uncertain reliability because of high $^{147}Sm/^{144}Nd$ (Table II).

Discussion

The data presented here show that metavolcanic rocks of FM have widely varied compositions. Several groups have been distinguished, with considerable differences in major and trace element contents and ratios. Although there is evidence for secondary redistribution of some elements (LILE and probably LREE), less mobile elements (such as HFSE) show consistent differences, considered to be primary, between groups. Hence, various processes (crystal fractionation/accumulation, different degrees of partial melting, crustal assimilation, source heterogeneity, etc.) have presumably played important roles in the petrogenesis of these rocks.

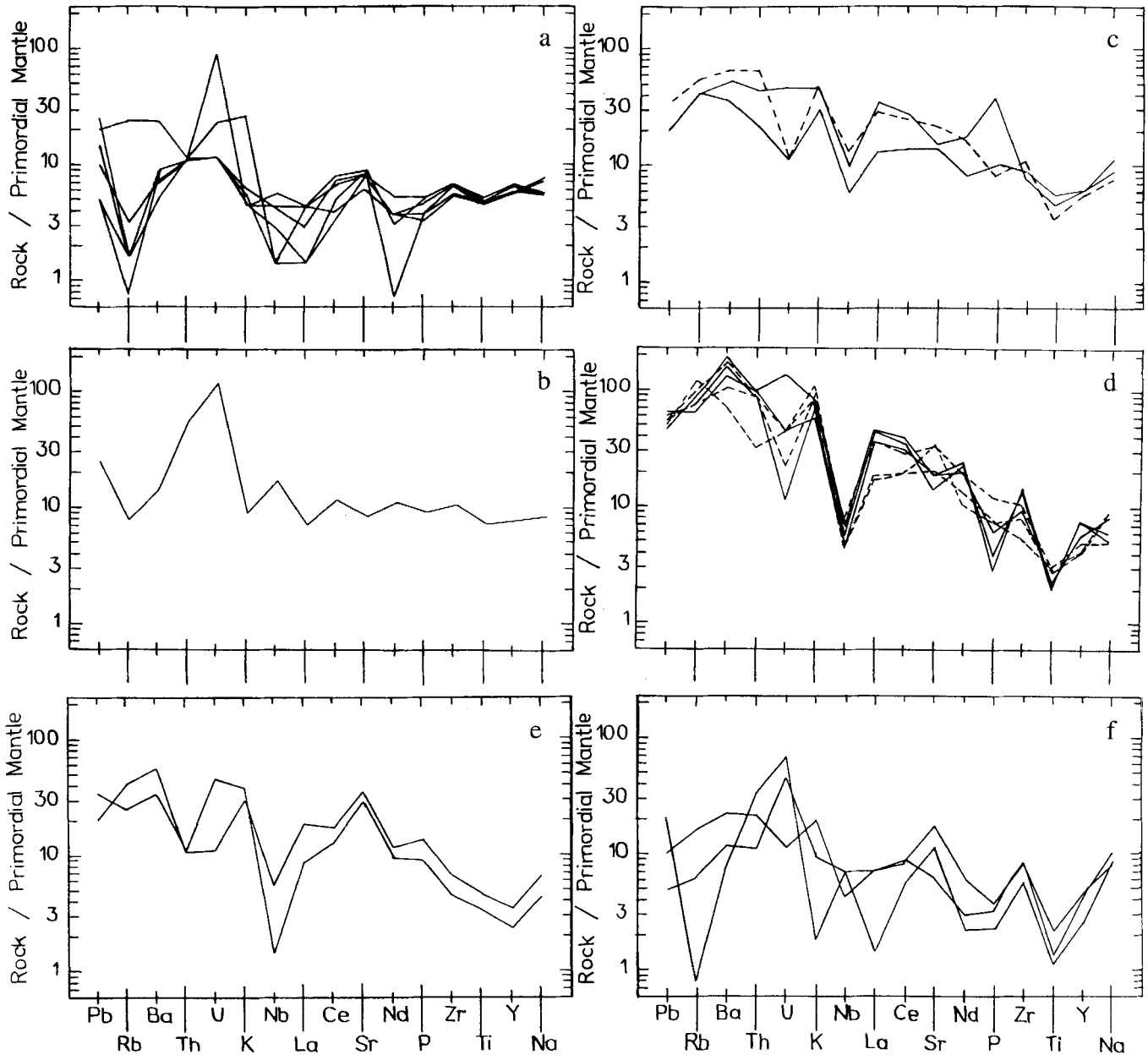

Fig. 8. Primordial mantle-normalized incompatible element abundance patterns (spidergrams). Normalization values from Sun & McDonough (1989). **a.** Group B1 basalts. **b.** Group B2 basalt. **c.** Group A1 basaltic andesites (solid lines) and andesite (dashed line). **d.** Group A2 andesites (dashed lines) and rhyolites (solid lines). **e.** Plagioclase porphyries (group PP). **f.** Felsic subvolcanic rocks.

https://doi.org/10.1017/S0954102096000120 Published online by Cambridge University Press

Crystal fractionation

Because of the very limited compositional variations and scatter of the data, partly due to alteration, the nature of possible fractionating phases for group B1 basalts must remain tentative. Marked decreases of Ni and Cr with *mg* decreasing from 58 to 53, and wide variations of MgO and Al_2O_3 with relatively small changes in SiO_2 suggest some degree of olivine and/or pyroxene fractionation. However, the lack of Sr depletion (Fig. 8a) does not allow much plagioclase fractionation; indeed, minor plagioclase accumulation could account for the negative correlation between MgO and CaO, and small positive Sr anomalies (Figs 8a & 9a).

Only one B2 basalt was analysed for trace elements and possible fractionating minerals cannot be identified with any confidence, except that fractionation of ferromagnesian minerals (and plagioclase?) must have occurred to produce low Ni, Cr, and *mg*, and minor Sr depletion (Fig. 8b). It is unlikely that significant differences in many incompatible element ratios between B1 and B2 basalts are due to fractionation, even though the latter are slightly more evolved. Some of the relative enrichment of group B2 could be due to lower percentage melting, but a distinct, somewhat more enriched (e.g. higher Nb/Zr), source is nevertheless required.

Plagioclase porphyries (PP) show positive Zr-TiO_2, Zr-Nb, and Zr-Y correlations (and a negative Zr-MgO correlation), consistent with fractional crystallization during which these minor elements behaved incompatibly. In contrast, the strong negative correlation of Sr with Zr (Fig. 10), along with marked positive Sr anomalies (Fig. 8e), show that Sr was far from incompatible and that plagioclase accumulation was an important process.

Group A1 rocks show only poorly-defined trends for most major elements on SiO_2 variation diagrams (Fig. 5). The basaltic andesites can be divided into high-Al_2O_3 (16–18%) and low-Al_2O_3 (14–15%) subgroups. The latter subgroup shows an initial positive correlation of Al_2O_3 with SiO_2, which could be due to crystal fractionation dominated by ferromagnesian phases (olivine + clinopyroxene). At later stages, fractionation involving major plagioclase is supported by decreasing Al_2O_3 and negative Zr-Sr and Zr-Ba correlations

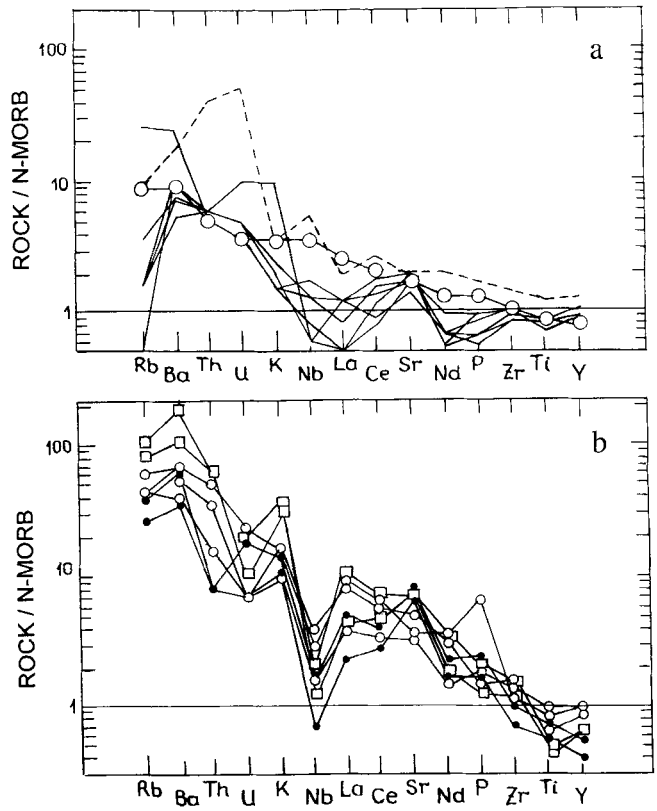

Fig. 9. N-MORB normalized spidergrams. Normalization values from Sun & McDonough (1989). **a.** Group B1 basalts (solid lines); group B2 basalt (dashed line); P-MORB (○). **b.** Group PP (•), group A1 (○), group A2 andesites (□).

(Fig. 10). The high-Al compositions cannot be explained in terms of plagioclase accumulation, because plagioclase phenocrysts are lacking, and one sample (36812–14) has a negative Sr anomaly (Fig. 8c). In contrast, two low-Al samples have small positive Sr anomalies and the more siliceous of these (36812–20) has relatively high *mg*. All these features indicate the presence of several distinct magma types (assuming no major alteration effects), and hence distinct parent magmas, and probably different source compositions, are implied.

Table II. Isotopic data for volcanic rocks and granodiorites from Fisher Massif.

	Field number	Rb [ppm]	Sr [ppm]	$^{87}Rb/^{86}Sr$	$^{87}Sr/^{86}Sr$	Sm [ppm]	Nd [ppm]	$^{147}Sm/^{144}Nd$	$^{143}Nd/^{144}Nd$	Sr_i	Nd_{DM} Ma	ε(Nd) T=1300
1	34516-1	17.51	214.56	0.23612	0.708520	6.44	27.13	0.14336	0.512265	0.7041	1940	+1.6
2	31030-2	14.42	393.31	0.10610	0.705468	2.77	11.35	0.14765	0.512347	0.7035	1870	+2.5
3	31026-1	115.8	145.06	2.31491	0.729166	1.63	5.76	0.17143	0.512534	0.686	2250	+2.2
4	33047	136	309	1.3648	0.72287	5.03	26.45	0.11503	0.512060	0.7059	1700	+2.4
5	33047-1	120	349	1.0755	0.71978	4.75	26.33	0.10914	0.512035	0.7059	1640	+2.8
6	33047-4	113	406	0.8445	0.71641	4.33	22.84	0.11473	0.512095	0.7064	1640	+3.0

1 = group A2 dacite, 2 = plagioclase porphyry, 3 = group A1 basaltic andesite, 4–6 = granodiorites.
Constants used: $^{143}Nd/^{144}Nd(CHUR) = 0.512636$, $^{147}Sm/^{144}Nd(CHUR) = 0.1967$, $^{143}Nd/^{144}Nd(DM) = 0.51316$, $^{147}Sm/^{144}Nd(DM) = 0.2136$.

https://doi.org/10.1017/S0954102096000120 Published online by Cambridge University Press

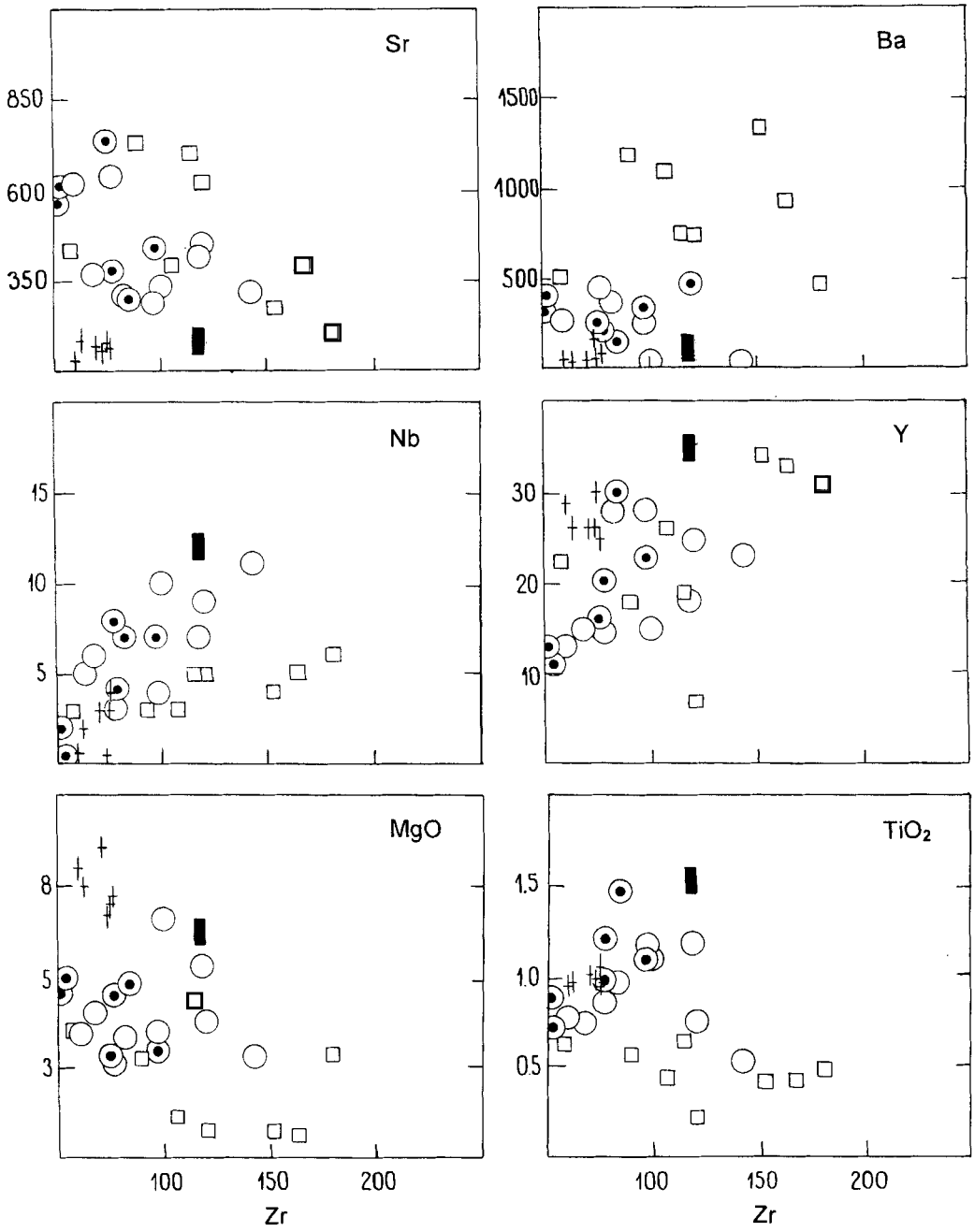

Fig. 10. Zr - trace element plots. Symbols as in Fig. 5.

Rocks of group A2 show negative correlations of FeO_{total}, MgO, CaO, and Al_2O_3 with SiO_2 (Fig. 5), consistent with low-pressure fractionation involving major plagioclase. Relatively constant Na_2O and K_2O contents also imply that fractionation of alkali-rich phases (plagioclase and possibly, in the more felsic rocks, K-feldspar) occurred. Petrographical data support this suggestion. Fractionation of a Ti-rich phase (probably ilmenite) was also important (Fig. 10). Spidergrams (Fig. 8d) appear to be generally consistent with the felsic group A2 rocks having formed by fractionation, possibly through AFC (assimilation–fractional crystallization: DePaolo 1981) processes, of an intermediate (andesitic) magma (large negative P and Ti anomalies, and smaller negative Sr anomalies in rhyolites). However, fractionation of an A2 andesitic magma is unlikely, because, unlike the felsic rocks, they are of high-K type. Alternatively, formation of the felsic rocks by partial melting of lower crustal material is quite possible.

Crustal contamination

The relatively smooth, flat spidergram patterns (apart from some LILE) of B1 and B2 basalts (Fig. 8a &b) do not support extensive crustal contamination of the basaltic magmas, in spite of their low-P and Ti character. In particular, the lack of significant LREE enrichment and Nb depletion, along

https://doi.org/10.1017/S0954102096000120 Published online by Cambridge University Press

with low La/Nb ratios (<1), preclude any major role for crustal contamination (Thompson *et al.* 1984), although minor LILE contamination cannot be discounted.

In contrast, groups PP, A1 and A2 have many features which could be due to significant degrees of contamination. Thus, the more primitive basaltic andesites of these groups have marked negative Nb anomalies and LILE and LREE enrichment, reflected by high La/Nb ratios (>2). However, an appropriate contaminant which satisfies available Rb-Sr and Sm-Nd data is not easy to find. For instance, simple mass-balance calculations show that 10–15% (groups PP, A1) and as much as 40% (group A2) of Archaean RT granitic crust (ε^0_{Nd} = -24 to -37, Fig. 11; V. P. Kovach, unpublished data) would need to have been assimilated by a depleted-mantle (DM) source to yield the observed ε_{Nd} values. If a younger (e.g., 1800–2000 Ma), and hence radiogenic Nd-enriched, felsic crustal contaminant is assumed, then even larger amounts of assimilation would be required. A more likely model would involve derivation of all three basaltic andesite-dacite groups (PP, A1, A2) from enriched mantle sources, although quite probably with significant additional crustal contamination. More data are clearly needed to investigate the possible importance of AFC processes. However, it may still be difficult to distinguish between generation of magma from an enriched mantle source in which the crustal component was derived from subducted oceanic crust and associated sediments, and more direct crustal assimilation (Sheraton *et al.* 1990).

Source heterogeneity

Chemical data imply different mantle sources for the two basaltic groups B1 and B2. The former was apparently derived from a depleted mantle source, which is shown by low LREE and HFSE contents broadly similar to N-MORB. Degrees of partial melting for B1 magmas (low K and Zr, high MgO) were presumably fairly large (at least 10%), so that, contamination and alteration effects apart, incompatible elements should not have been significantly fractionated during melting, and thus ratios of such elements should essentially reflect those of the mantle source. Chondrite-normalized $(La/Ce)_N$ and, in some cases, $(Ce/Nd)_N$ and $(Ce/Y)_N$ of less than unity may partly be due to alteration, but, along with high Zr/Nb (19–31), indicate a source region having features of depleted mantle. However, present-day N-MORB has lower Ba/Zr (0.085) and higher Zr/Rb (132) and K/Ba (95) ratios and lower LILE contents (Fig. 9) (Sun & McDonough 1989). Relatively high LILE may either be due to the presence of a subduction-related component in the source or to small degrees of crustal contamination. Arculus & Powell (1986) showed that Ba/La ratios are typically higher in island-arc basalt (IAB) (mostly 5–70) compared to MORB and intra-plate basalt (generally <20). Thus, if the high Ba/La ratios of the B1 rocks (17–20) are essentially primary (i.e. are not due to alteration or analytical uncertainties), they may well reflect metasomatic enrichment of the mantle wedge by fluids or partial melts derived from subducted oceanic sediments (Hole *et al.* 1984). Group B1 may therefore represent a low-K volcanic arc tholeiitic suite, typical of subduction-related equivalents of MORB.

The group B2 basalt was apparently derived from a somewhat different mantle source region, more akin to P-MORB with higher Zr, Nb, LREE, and LILE contents, higher $(Ce/Y)_N$ (1.5), and lower La/Nb and Zr/Nb. It is possible that some of this greater incompatible element enrichment is due to somewhat greater fractionation and/or smaller degrees of partial melting, but neither can account for all the observed differences. The appearance of group B2 higher in the volcanic succession (the lower part of sequence 3), assuming that the sequence is overturned, implies a complex magmatic evolution, perhaps involving a less-depleted, more Nb-rich OIB-like component at a later stage, although more data would be needed to confirm this. The anomalously high Th and U contents and low Th/U of B2 sample 36811–19 (Fig. 8b) are unlikely to be mantle source characteristics, but may be due to interaction of the magma with a subduction-derived hydrous fluid phase in which U was more soluble than Th (Bailey & Ragnarsdottir 1994). More probably, they may merely reflect alteration.

Plagioclase porphyries, though highly fractionated, show significant differences from groups B1 and B2 in most trace

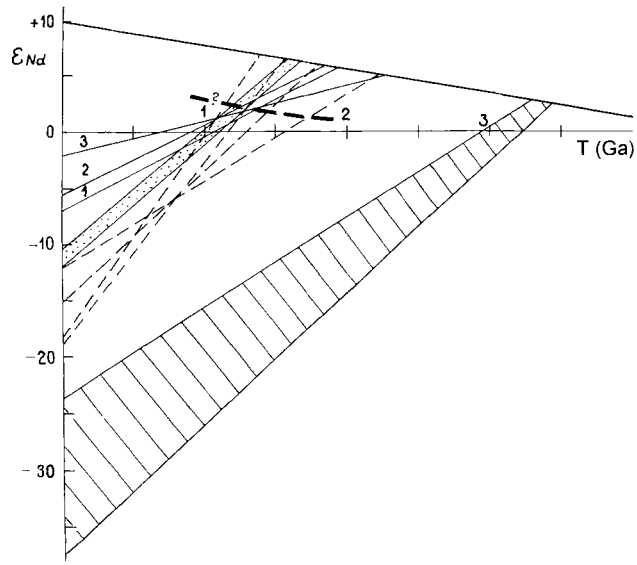

Fig. 11. ε Nd evolution diagram. Ruled field = RT granites and granite gneisses (V. P. Kovach, unpublished data), stippled field = FM granodiorites (this paper), dashed lines = NPCM granites (Manton *et al.*1992), solid lines = FM metavolcanic rocks. 1 = group A2 dacite (34516-1), 2 = plagioclase porphyry (31030-2), 3 = group A1 basaltic andesite (31026-1), heavy solid line = DM evolution trend from DePaolo (1981), heavy dashed line = possible mantle source of FM volcanics.

https://doi.org/10.1017/S0954102096000120 Published online by Cambridge University Press

element ratios, especially those involving LILE. As these rocks contain abundant plagioclase megacrysts, Ba and particularly Sr are not likely to have behaved incompatibly. Large positive Sr anomalies (Fig. 8e) reflect the presence of cumulus plagioclase. Nevertheless, the strong LILE enrichment of PP rocks cannot be due to plagioclase accumulation in a melt derived by fractionation of a B1-like parent magma. PP rocks have prominent negative Nb anomalies, and Zr/Y and P/Zr ratios are higher than those of groups B1 and B2. Assuming that they are not entirely due to fractionation, the low Y and Ti contents (Figs 7e & 9b) suggest derivation from a depleted (refractory?) source region, which subsequently underwent enrichment in LILE and LREE. It is possible that the enrichment event was co-eval with magma generation, i.e., by interaction with subduction-derived fluids. If so, the calculated model age (1870 Ma) would be meaningless.

Andesitic rocks of both groups A1 and A2 have large negative Nb anomalies, generally small positive Sr anomalies, high LILE/LREE, and low Ti and Y (Figs 8 & 9), all of which suggest derivation from generally similar source regions. Nevertheless, group A2 high-K andesites are more LILE-enriched and have distinctive incompatible element ratios (e.g. lower Ti/Zr) which suggest derivation from a slightly different source region to that of group A1. It is unlikely that these rocks originated from 'pure' mantle sources, but rather include both mantle (?DM) and LILE-rich crustal (probably at lest partly subduction-related) components, as was proposed for the PP rocks.

Relatively low ASI values of group A2 felsic rocks are consistent with derivation from igneous precursors. Group A2 rhyodacites and rhyolites have very irregular spidergrams which could have been produced by (AFC?) fractionation of plagioclase, ilmenite, apatite, and ferromagnesian phases from an andesitic parent magma. Alternatively, these rocks may have been derived by melting of felsic-intermediate crust, although the relatively small negative Sr anomalies are more difficult to explain by such a process. More isotopic data are needed to resolve these alternatives, but, in either case, a significant continental crustal component is likely.

Felsic subvolcanic rocks are markedly K-poor and probably represent yet another magma type. The limited geochemical data suggest that they are not directly related to any of the volcanic groups. Neither is there any clear compositional correlation between the felsic volcanic and granitic rocks (Sheraton *et al.* in press), which appear to have consistently older Nd_{DM} model ages (Table II).

Palaeotectonic environment

A number of workers have suggested the use of various major and trace element plots to classify young basaltic or granitic rocks in terms of their tectonic environment. Caution must obviously be exercized when applying this approach to ancient igneous rocks, particularly altered ones. However, FM metavolcanic rocks do not appear to have suffered extensive HFSE mobility, which was probably mostly confined to LILE and, to some extent, LREE. Hence, plots involving

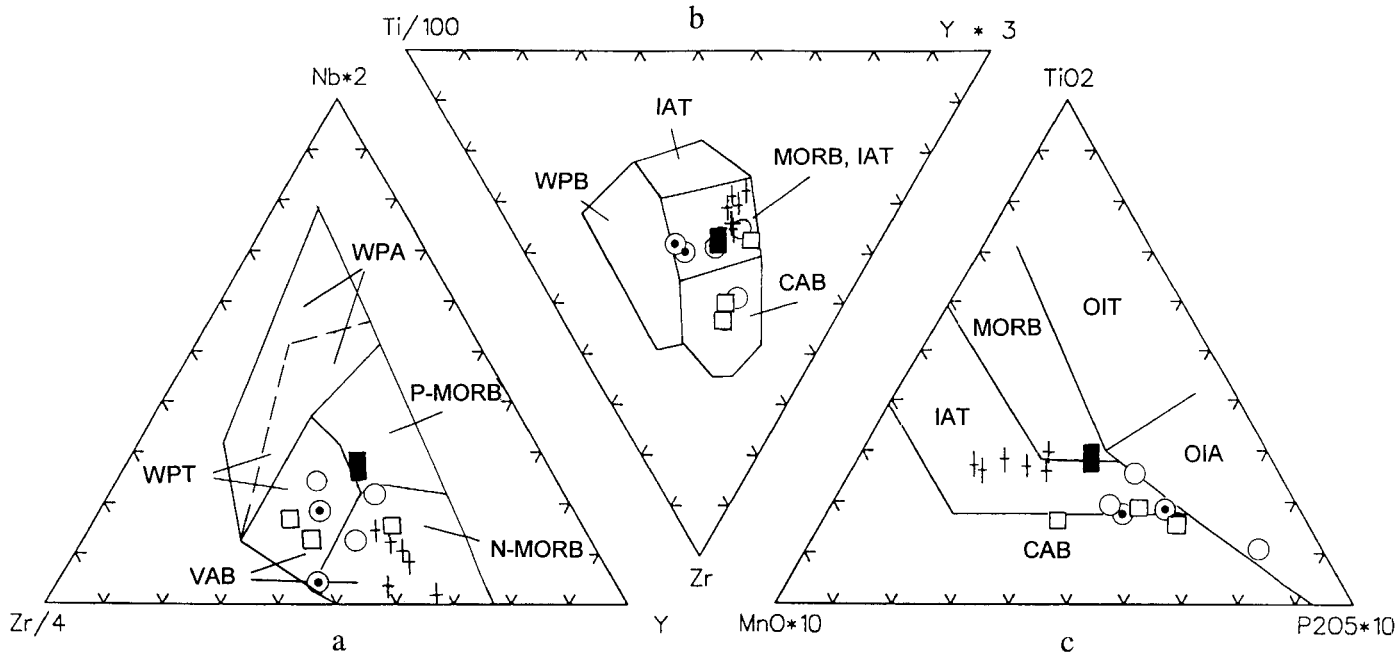

Fig. 12. a. Zr/4 - 2Nb- Y (Meschede 1986). **b.** Zr - Ti/100 - 3Y (Pearce & Cann 1973). **c.** 10MnO - TiO_2 - $10P_2O_5$ (Mullen 1983) variation diagrams. WPT = within plate tholeiite, VAB = volcanic arc basalt, WPA = within-plate alkaline basalt, MORB = mid ocean ridge basalt, WPB = within-plate basalt, IAT = island arc tholeiite, CAB calc-alkaline island arc basalt, OIT = ocean island tholeiite, OIA = ocean island alkali basalt. Symbols as in Fig. 5, except that only andesitic rocks of groups A1 and A2 are plotted.

https://doi.org/10.1017/S0954102096000120 Published online by Cambridge University Press

Nb, Zr, Y and Ti, which are believed to be relatively immobile during low-temperature alteration (Wilson 1989), may be useful (Rollinson 1993), particularly if geological evidence is also taken into account.

On triangular variation diagrams Zr/4-2Nb-Y (Meschede 1986), Zr-Ti/100-3Y (Pearce & Cann 1973), and 10MnO-TiO_2-10P_2O_5 (Mullen 1983), B1 and B2 basalts plot within the partly overlapping volcanic-arc/island-arc and MORB fields, but well outside the within-plate basalt fields (Fig. 12). On the last plot, group B1 samples fall outside the MORB field, although they have some chemical affinities with N-MORB, whereas group B2 is more like P-MORB. Intermediate rocks of groups A1 and A2 also have island-arc calc-alkaline characteristics. These plots thus support the suggestion that at least some FM metavolcanic rocks originated from subduction-modified mantle sources, which are characteristic of island-arc or active continental margin (Andean) environments. Moreover, felsic group A2 rocks have the low Rb, Y and Nb contents characteristic of volcanic-arc, rather than collisional, within-plate, or ocean ridge, granitoids on the classification of Pearce *et al.* (1984). Similarly, most FM granitoids also have volcanic-arc type compositions (Sheraton *et al.* in press).

FM volcanic rocks show a continuous range of SiO_2 contents, with a peak at basaltic compositions (Fig. 4), as well as a calc-alkaline evolutionary trend (Fig. 13), both typical of magmas produced at convergent plate margins. However, the distinct trends shown by many other, particularly trace, elements may be due to the presence of several different rock series, i.e., tholeiitic island-arc basalts and calc-alkaline to high-K calc-alkaline volcanic rocks. The present study has not provided unequivocal evidence for an ancient crustal component, but zircon U-Pb data for felsic volcanic rocks from FM reported by Beliatsky *et al.* (1994), including a model $^{207}Pb/^{206}Pb$ age of 2560 Ma for an A2 tuffaceous rhyodacite, suggest that it is likely. Moreover, a single 1900 Ma zircon xenocryst was found in a FM metadacite sample, and paragneiss from Mount Meredith (about 20 km north of FM) contains both Archaean (2500–2800 Ma) and Palaeoproterozoic (1600–2100 Ma) zircons (Kinny *et al.* in press). Hence, a continental block (possibly the RT) may well have been involved in the tectonic processes. The relative abundance of felsic rocks compared to typical island arcs (Wilson 1989) is also consistent with major continental crustal involvement in a continental arc (Andean plate margin).

Sheraton *et al.* (in press) postulated that an Andean plate margin which existed in the NPCM area about 1300 m.y. ago may have evolved into one of continental collision (possibly between the Archaean cratonic blocks, with probable Palaeoproterozoic components, of the SPCM and India) by 1000 Ma. If so, the FM rocks, which clearly escaped the 1000 Ma granulite-facies event which is characteristic of most of the NPCM, must have been at a much shallower crustal level at that time. The similarity in ages of younger

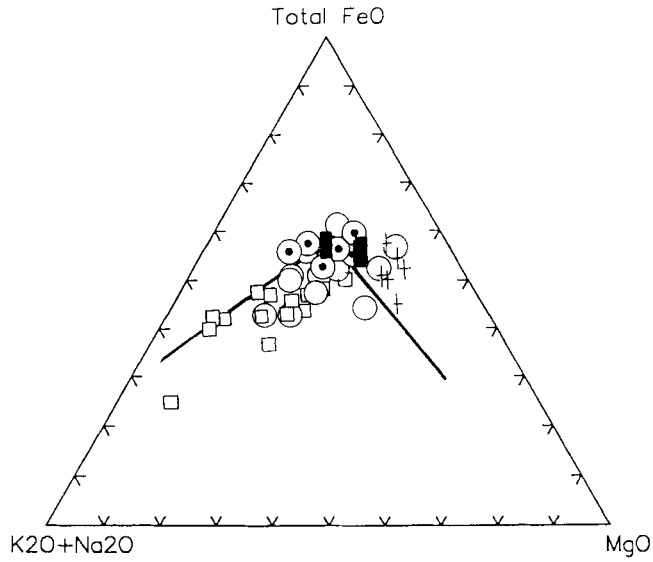

Fig. 13. A (Na_2O+K_2O) - F (total Fe as FeO) - M (MgO) diagram (wt. %). Dividing line between tholeiitic (upper) and calc-alkaline volcanic fields from Irvine & Baragar (1971). Symbols as in Fig. 5.

granites at FM to granitoids (including charnockitic types) elsewhere in the NPCM (Kinny *et al.* in press) and the broad similarity in Nd_{DM} model ages for rocks from both areas are consistent with them having originated at about the same time in the same plate margin. Alternatively, it is quite possible that the FM area represents a distinct microplate, which would account for its different compositional and structural features. Such a microplate would apparently include both Mount Willing, where a large metagabbro intrusion crops out, and Mount Meredith, as no evidence for a granulite-facies event has been found at either locality.

If many of the FM granitic and volcanic rocks represent new continental crust, as is suggested by chemical data, then their much older Nd_{DM} model ages (1600–2200 Ma; Table II) cannot be crustal formation ages, and are presumably due to mantle enrichment before or during magma generation and/or assimilation of older (?Archaean) crustal material. Similar Nd_{DM} model ages of granulite-facies gneisses in the NPCM (1800–2200 Ma: Hensen *et al.* 1992, S-S. Sun unpublished data) may also be misleadingly old, and these rocks could have been derived, at least in part, from Mesoproterozoic, rather than Palaeo proterozoic, protoliths (either directly or, in the case of metasedimentary rocks, through weathering). Nevertheless, significant amounts of Archaean to Palaeoproterozoic crust were clearly involved in the formation of the NPCM rocks, as 1600 to 2800 Ma inherited zircons have been found (L.P. Black, personal communication 1995).

Although the possibility that FM represents a distinct microplate certainly cannot be discounted, it is quite possible that at least some of the protoliths of the high-grade, mostly felsic orthogneisses were formed in the same Andean plate margin as the FM igneous rocks. The relative abundance of

mafic to intermediate rocks at FM could reflect differences in the maturity of the arc during magma generation, differences in crustal level at that time, or a combination of both. Some of the widespread mafic granulite layers in the high-grade terrane are probably metamorphosed dykes which could have been feeders to a volcanic pile. Moreover, continental arcs are likely to be tectonically highly complex, with the type of magmatism dependent on the nature of the associated deformation (compression during periods of active subduction, or extension) which can vary in both space and time (Soler & Bonhomme 1990). This is particularly the case with terranes as extensive as the PMB, which is difficult to reconcile with formation at a single convergent plate margin (Stüwe & Hand 1992). Indeed, the PMB apparently forms part of global-scale mobile belt of Grenvillian age (Moores 1991, Dalziel 1991).

Conclusions

The lithological and chemical compositions of FM metavolcanic sequences show that several different source materials were involved in a complex sequence of magma generation. Assuming that the succession exposed in the Kar Bolshoi area is overturned, then group B1 basaltic rocks would be the oldest. These rocks are likely to have originated from a subduction-modified depleted mantle source region, possibly in an island arc or back-arc basin. Rocks of the mostly andesitic group A1 are believed to have been derived from a distinct mantle source, with a more significant additional (either partly or wholly subduction-derived) crustal component. They originated before the cessation of the earlier mantle melting, and rocks of both basaltic and andesitic composition are commonly intercalated. At a later stage, somewhat more evolved melts (B2 basalts) of a relatively Nb-rich P-MORB or OIB-like mantle source appeared, perhaps generated in a back-arc marginal basin environment. Intermediate-felsic medium to high-K volcanic rocks of group A2 postdate the main basaltic successions, probably reflecting a more evolved stage of arc activity with greater crustal invovement in a continental margin. High-Al plagioclase porphyries (PP) appear to terminate the volcanic activity, and were derived from a mantle (+ crustal) source broadly similar to those of the groups A1 and A2 andesitic rocks. Groups A1, A2 and PP rocks belong to several distinct suites of calc-alkaline character. Such a progression from predominantly tholeiitic to calc-alkaline volcanics is typical of the evolution of island arcs (Wilson 1989, Yanagi & Yamashita 1994).

Determining the tectonic environment of such a complex volcanic sequence, the present geological setting of which is ambiguous and which has subsequently been metamorphosed, is clearly full of pitfalls. Nevertheless, an active continental margin with an associated island arc appears best to fit the limited data available for the FM volcanic rocks. The FM volcanic rocks probably represent Mesoproterozoic (*c.*1300 Ma) mantle-derived additions to crust, together with subduction-derived and older (including Archaean) felsic crustal components. They may either represent a higher crustal level of the PMB or a distinct microplate. Prior to both the FM magmatism and that in which the protoliths of NPCM orthogneisses were derived from the mantle (probably also at least partly in the Mesoproterozoic), an oceanic basin capable of producing subduction zones presumably existed in the present Prince Charles Mountains area. Hence, the initial evolution of the PMB and its relations to the RT may be considered in terms of a convergent lithospheric plate margin. The presence of dolerite dyke swarms of broadly similar age in the Vestfold Hills (1380 and 1240 Ma: Lanyon *et al.* 1993) and probably the SPCM (Sheraton *et al.* 1987) suggests that crustal extension processes responsible for dyke emplacement in the cratonic blocks and subduction-related processes in the adjacent mobile belt may have been roughly co-eval.

Acknowledgements

The authors are grateful to Drs E. Kamenev, D. Krylov, A. Andronikov and S-S. Sun for fruitful discussions, to Natalia Zanegina and Lindell Emerton for drawing the figures and to A. Melnik and D. Krylov for field assistance. Shen-Su Sun and Bob Tingey provided invaluable comments on the manuscript, which was also much improved thanks to careful reviews by Keith Cox and David Elliot. The research described here was made possible in part by grant R14000 from the International Science Foundation. JWS publishes with the permission of the Executive Director, AGSO.

References

Arculus, R.J. & Powell, R. 1986. Source component mixing in the regions of arc magma generation. *Journal of Geophysical Research*, **91**, 5913–5926.

Bailey, E.H. & Ragnarsdottir, K.V. 1994. Uranium and thorium solubilities in subduction zone fluids. *Earth and Planetary Science Letters*, **124**, 119–129.

Beliatsky, B.V., Laiba A.A. & Mikhalsky, E.V. 1994. U-Pb zircon age of the metavolcanic rocks of Fisher Massif (Prince Charles Mountains, East Antarctica). *Antarctic Science*, **6**, 355–358.

Black, L.P., Sheraton, J.W. & Kinny, P.D. 1992. Archaean events in Antarctica. *In* Yoshida, Y., Kaminuma, K. & Shiraishi, K., *eds. Recent progress in Antarctic earth science*. Tokyo: Terra Scientific Publishing Company, 1–6.

Collerson, K.D. & Sheraton, J.W. 1986. Age and geochemical characteristics of a mafic dyke swarm in the Archaean Vestfold Block, Antarctica: inferences about Proterozoic dyke emplacement in Gondwana. *Journal of Petrology*, **27**, 853–886.

Cox, K.G., Bell, J.D. & Pankhurst, R.J. 1979. *The interpretation of igneous rocks*. London: George Allen and Unwin, 450 pp.

Crohn, P.W. 1959. A contribution to the geology and glaciology of the western part of Australian Antarctic Territory. *Bureau of Mineral Resources, Australia, Bulletin*, No. 52, 103pp.

Dalziel, I.W.D. 1991. Pacific margins of Laurentia and East Antarctica-Australia as a conjugate rift pair: evidence and implications for an Eocambrian supercontinent. *Geology*, **19**, 598–601.

DePaolo, D. 1981. Trace element and isotopic effects of combined wallrock assimilation and fractional crystallisation. *Earth and Planetary Science*

Letters, **53**, 189–202.

FITZSIMONS, I.C.W. & HARLEY, S.L. 1992. Mineral reaction textures in high-grade gneisses: evidence for contrasting pressure-temperature paths in the Proterozoic complex of East Antarctica. *In* YOSHIDA, Y., KAMINUMA, K. & SHIRAISHI, K., *eds. Recent progress in Antarctic earth science.* Tokyo: Terra Scientific Publishing Company, 103–111.

FITZSIMONS, I.C.W. & THOST, D.E. 1992. Geological relationships in high-grade basement gneiss of the northern Prince Charles Mountains, East Antarctica. *Australian Journal of Earth Sciences*, **39**, 173–193.

HARLEY, S.L. 1988. Proterozoic granulites from the Rauer Group, East Antarctica. I. Decompressional pressure-temperature paths deduced from mafic and felsic gneisses. *Journal of Petrology*, **29**, 1059–1095.

HARLEY, S.L., FITZSIMONS, I.C.W., BUICK, I.S. & WATT, G. 1992. The significance of reworking, fluids and partial melting in granulite metamorphism, east Prydz Bay, Antarctica. *In* YOSHIDA, Y., KAMINUMA, K. & SHIRAISHI, K., *eds. Recent progress in Antarctic earth science.* Tokyo: Terra Scientific Publishing Company, 119–127.

HENSEN, B.J. & ZHOU, B. 1995. A Pan-African granulite facies metamorphic episode in Prydz Bay, Antarctica: evidence from Sm-Nd garnet dating. *Australian Journal of Earth Sciences*, **42**, 249–258.

HENSEN, B.J., MUNKSGAARD, N.C. & THOST, D.E. 1992. Geochemistry and geochronology of Proterozoic granulites from the northern Prince Charles Mountains, East Antarctica. *ANARE Research Notes*, **85**, 9.

HOLE, M.J., SAUNDERS, A.D., MARRINER, G.F. & TARNEY, J. 1984. Subduction of pelagic sediments: implications for the origin of Ce-anomalous basalts from Mariana Islands. *Journal of the Geological Society, London*, **141**, 453–472.

IRVINE, T.N. & BARAGAR, W.R.A. 1971. A guide to the chemical classification of the common volcanic rocks. *Canadian Journal of Earth Sciences*, **8**, 523–548.

KAMENEV, E.N. 1991. Structure and evolution of Precambrian cratons and metamorphic belts in East Antarctica. *Sixth International Symposium on Antarctic Earth Sciences, National Institute of Polar Research, Tokyo, 9-13 September, 1991.* Abstract volume, 261–263.

KAMENEV, E.N. 1993. Structure and evolution of the Antarctic shield in Precambrian. *In* FINDLEY, R.H., UNRUG, R., BANKS, M.R. & VEEVERS, J.J., *eds. Gondwana eight: assembly, evolution and dispersal.* Rotterdam: A.A. Balkema, 141–151.

KAMENEV, E., ANDRONIKOV, A.V., MIKHALSKY E.V., KRASNIKOV, N.N. & STÜWE, K. 1993. Soviet geological maps of the Prince Charles Mountains, East Antarctic Shield. *Australian Journal of Earth Sciences*, **40**, 501–517.

KINNY, P.D., BLACK, L.P. & SHERATON, J.W. In press. Zircon U-Pb ages and geochemistry of igneous and metamorphic rocks from the northern Prince Charles Mountains, Antarctica. *AGSO Journal of Australian Geology and Geophysics*.

KOVACH, V.P. & BELIATSKY, B.V. 1991. Geochemistry and age of granitic rocks in the Ruker granite-greenstone terrain, southern Prince Charles Mountains, East Antarctica. *Sixth International Symposium on Antarctic Earth Sciences, National Institute of Polar Research, Tokyo, 9–13 September*, 1991. Abstract volume, 321–326.

KRASNIKOV, N.N. & FEDOROV, L.V. 1992. Geologicheskoe stroenie massiva Fisher, Vostochnaya Antarctida. [Geological structure of Fisher Massif, East Antarctica.] *Izvestia Akademii Nauk SSSR, Earth-Science Section*, **8**, 123–134.

LANYON, R., BLACK, L.P. & SEITZ, H-M. 1993. U-Pb zircon dating of mafic dykes and its application to the Proterozoic geological history of the Vest fold Hills, East Antarctica. *Contributions to Mineralogy and Petrology*, **115**, 184–203.

LE MAITRE, R.W. 1989. *A classification of igneous rocks and glossary of terms.* Oxford: Blackwell Scientific Publications, 193 pp.

MANTON, W.I., GREW, E.S., HOFMANN, J. & SHERATON, J.W. 1992. Granitic rocks of the Jetty Peninsula, Amery Ice Shelf area, East Antarctica. *In* YOSHIDA, Y., KAMINUMA, K. & SHIRAISHI, K., *eds. Recent progress in Antarctic earth science.* Tokyo: Terra Scientific Publishing Company, 179–189.

MCLEOD, I.R. 1964. An outline of the geology of the sector from longitude 45° to 80° E, Antarctica. *In* ADIE, R.J., *ed. Antarctic geology*. Amsterdam: North-Holland Publishing Company, 237–247.

MESCHEDE, M. 1986. A method of discriminating between different types of mid-ocean ridge basalts and continental tholeiites with the Nb-Zr-Y diagram. *Chemical Geology*, **56**, 207–218.

MIDDLEMOST, E.A.K. 1975. The basalt clan. *Earth-Science Reviews*, **11**, 337–364.

MIKHALSKY, E.V. 1993. Petrohimicheskaya haracteristica izverzhennjh porod massiva Fisher (Vostochnaya Antarctida). [Petrochemical characteristics of igneous rocks from Fisher Massif (East Antarctica).] *Antarktica*, **32**, 41–57.

MIKHALSKY, E.V., ANDRONIKOV, A.V., BELIATSKY, B.V. & KAMENEV, E.N. 1993. Mafic igneous suites in the Lambert rift zone. *In* FINDLEY, R.H., UNRUG, R., BANKS, M.R. & VEEVERS, J.J., *eds. Gondwana eight: assembly, evolution and dispersal.* Rotterdam: A.A. Balkema, 541–546.

MIYASHIRO, A. 1978. Nature of alkalic volcanic rock series. *Contributions to Mineralogy and Petrology*, **66**, 91–104.

MOORES, E.M. 1991. Southwest U.S.-East Antarctica (SWEAT) connection: a hypothesis. *Geology*, **19**, 425–428.

MULLEN, E.D. 1983. $MnO/TiO_2/P_2O_5$: a minor element discriminant for basaltic rocks of oceanic environments and its implication for petrogenesis. *Earth and Planetary Science Letters*, **62**, 53–62.

MUNKSGAARD, N.C., THOST, D.E. & HENSEN, B.J. 1992. Geochemistry of Proterozoic granulites from northern Prince Charles Mountains, East Antarctica. *Antarctic Science*, **4** 59–69.

NORRISH, K. & CHAPPELL, B.W. 1977. X-ray fluorescence spectrometry. *In* ZUSSMAN, J., *ed. Physical methods in determinative mineralogy.* London: Academic Press, 201–272.

NORRISH, K. & HUTTON, J.T. 1969. An accurate X-ray spectrographic method for the analysis of a wide range of geological samples. *Geochimica et Cosmochimica Acta*, **33**, 431–453.

OLIVER, R.L., JAMES, P.R., COLLERSON, K.D. & RYAN, A.B. 1982. Precambrian geologic relationships in the Vestfold Hills, Antarctica. *In* CRADDOCK, C., *ed. Antarctic geoscience.* Madison: University of Wisconsin Press, 435–444.

PEARCE, J.A. & CANN, J.R. 1973. Tectonic setting of basic volcanic rocks determined using trace element analyses. *Earth and Planetary Science Letters*, **19**, 290–300.

PEARCE, J.A., HARRIS, N.B.W. & TINDLE, A.G. 1984. Trace element discrimination diagrams for the interpretation of granitic rocks. *Journal of Petrology*, **25**, 956–983.

PERCHUK, L.L., ARANOVICH, L.YA., PODLESSKII, K.K., LAVRANT'EVA, I.V., GERASIMOV, V.YU., FED'KIN, V.V., KITSUL, V.I., KARSAKOV, L.P. & BERDNIKOV, N.V. 1985. Precambrian granulites of the Aldan Shield, eastern Siberia, USSR. *Journal of Metamorphic Geology*, **3**, 265–310.

RAVICH, M.G., SOLOVIEV, D.S. & FEDOROV, L.V. 1984. *Geological structure of MacRobertson Land (East Antarctica).* New Delhi: Amerind Publishing, 254 pp.

ROLLINSON, H. 1993. *Using geochemical data: evaluation, presentation, interpretation.* Harlow, Essex: Longman, 352 pp.

SHERATON, J.W. & COLLERSON K.D. 1984. Geochemical evolution of Archaean granulite-facies gneisses in the Vestfold Block and comparisons with other Archaean gneiss complexes in the East Antarctic Shield. *Contributions to Mineralogy and Petrology*, **87**, 51–64.

SHERATON, J.W., THOMSON, J.W. & COLLERSON K.D. 1987. Mafic dyke swarms of Antarctica. *In* HALLS, H.C. & FAHRIG W.F., *eds. Mafic dyke swarms.* Geological Association of Canada Special Paper, No. 34, 419–432.

SHERATON, J.W., TINDLE, A.G. & TINGEY, R.J. In press. Geochemistry, origin, and tectonic setting of granitic rocks of the Prince Charles Mountains, Antarctica. *AGSO Journal of Australian Geology and Geophysics*.

SHERATON, J.W., BLACK, L.P., MCCULLOCH, M.T. & OLIVER, R.L. 1990. Age and origin of a compositionally varied mafic dyke swarm in the Bunger Hills, East Antarctica. *Chemical Geology*, **85**, 215–246.

SOLER, P. & BONHOMME, M.G. 1990. Relation of magmatic activity to plate dynamics in central Peru from late Cretaceous to present. *In* KAY, S.M. & RAPELA, C.W., *eds. Plutonism from Antarctica to Alaska.* Geological Society of America Special Paper, No. 241, 173–191.

STÜWE, K. 1992. A review of the basement geology and our current knowledge thereof in the northern Prince Charles Mountains. *ANARE Research Notes*, **85**, 17–18.

STÜWE, K. & HAND, M. 1992. Geology and structure of Depot Peak, MacRobertson Land. More evidence for the continuous extent of the 1000 Ma event of East Antarctica. *Australian Journal of Earth Sciences*, **39**, 211–222.

STÜWE, K. & POWELL, R. 1989. Low-pressure granulite facies metamorphism in the Larsemann Hills area, East Antarctica; petrology and tectonic implications for the evolution of the Prydz Bay area. *Journal of Metamorphic Geology*, **7**, 465–483.

STÜWE, K., BRAUN, H-M. & PEER, H. 1989. Geology and structure of the Larsemann Hills area, Prydz Bay, East Antarctica. *Australian Journal of Earth Sciences*, **36**, 219–241.

SUN, S-S. & MCDONOUGH, W.F. 1989. Chemical and isotopic systematics of oceanic basalts: implications for mantle composition and processes. *In* SAUNDERS, A.D. & NORRY, M.J., *eds. Magmatism in the ocean basins.* Geological Society of London Special Publication, No. 42, 313–345.

TARNEY, J., WYBORN, L.E.A., SHERATON, J.W. & WYBORN, D. 1987. Trace element differences between Archaean, Proterozoic and Phanerozoic crustal components - implications for crustal growth processes. *In* ASHWAL, L.D., *ed. Workshop on the growth of continental crust.* Lunar and Planetary Institute, Technical Report 88.02, 139–140.

THOMPSON, R.N., MORRISON, M.A., HENDRY, G.L. & PARRY, S.J. 1984. An assessment of the relative roles of crust and mantle in magma genesis: an elemental approach. *Philosophical Transactions of the Royal Society of London*, **A310**, 549–590.

THOST, D.E. & HENSEN, B.J. 1992. Gneisses of the Porthos and Athos Ranges, northern Prince Charles Mountains, East Antarctica: constraints on the prograde and retrograde P-T path. *In* YOSHIDA, Y., KAMINUMA, K. & SHIRAISHI, K., *eds. Recent progress in Antarctic earth science.* Tokyo: Terra Scientific Publishing Company, 93–102.

TINGEY, R.J. 1974. Australian geological mapping in the Prince Charles Mountains, 1968–1973. *Polar Record*, **17**, 150–153.

TINGEY, R.J. 1982. The geologic evolution of the Prince Charles Mountains - an Antarctic Archean cratonic block. *In* CRADDOCK, C., *ed. Antarctic geoscience.* Madison: University of Wisconsin Press, 455–464.

TINGEY, R.J. 1991. The regional geology of Archaean and Proterozoic rocks in Antarctica. *In* TINGEY, R.J., *ed. The geology of Antarctica.* Oxford: Clarendon Press, 1–58.

WHITE, A.J.R. & CHAPPEL, B.W. 1983. Granitoid types and their distribution in the Lachlan Fold Belt, southeastern Australia. *In* RODDICK, J.A., *ed. Circum Pacific plutonic terranes.* Geological Society of America Memoir, No. 159, 21–34.

WILSON, M. 1989. *Igneous petrogenesis.* London: Chapman and Hall, 466 pp.

YANAGI, T. & YAMASHITA, K. 1994. Genesis of continental crust under island arc conditions. *Lithos*, **33**, 209–223.

ZHAO, Y., SONG, B., WANG, Y., REN, L., LI, J. & CHEN, T. 1992. Geochronology of the late granite in the Larsemann Hills, East Antarctica. *In* YOSHIDA, Y., KAMINUMA, K. & SHIRAISHI, K., *eds. Recent progress in Antarctic earth science.* Tokyo: Terra Scientific Publishing Company, 155–161.